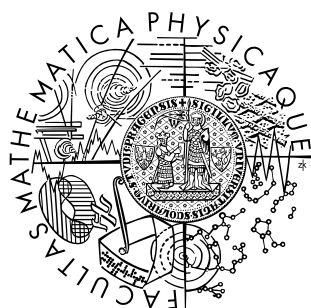


Univerzita Karlova v Praze
Matematicko-fyzikální fakulta

DIPLOMOVÁ PRÁCE



Matúš Kurian

Klasický chaos v geometrickém kolektivním modelu jader

Vedoucí diplomové práce: *Doc. RNDr. Pavel Cejnar, Dr.*

Studijní program: *Fyzika, Teoretická fyzika*

Poďakovanie Na tomto mieste by som rád spomenul ľuď, ktorí sa výrazne zaslúžili o to, že táto práca vznikla.

Prednostne by som chcel poďakovať Pavlovi Cejnarovi, ktorý ma k tejto téme priviedol a dohliadol na to, aby práca bola dokončená. Jeho rady a podnety boli neoceniteľné a často inšpirujúce. Zároveň chcem poďakovať Pavlovi Stránskému za jeho prácu, ktorá bola nielen motiváciou, ale aj užitočným zdrojom poučenia.

Za mnohé vďačím svojim kolegom a spolužiakom: Martinovi Fraasovi, Michalovi Mackovi, Davidovi Kofroňovi, Oldřichovi Kepkovi a Jiřímu Peškovi. Svojimi radami mi neraz pomohli nájsť kľúč k mnohým problémom.

Zároveň by chcel tu vyjadriť vďaku svojim rodičom.

Prohlašuji, že jsem svou diplomovou práci napsal samostatně a výhradně s použitím citovaných pramenů. Souhlasím se zapůjčováním práce.

V Praze dne 2.9.2005

Matůš Kurian

Contents

1	Introduction	1
1.1	Overview	1
1.2	Bibliographical Notes	6
2	The Kinematics of the GCM	7
2.1	Basics	7
2.2	Quadrupole Deformations and the Principal Axes System . . .	8
2.2.1	The Bohr Coordinates	10
3	The Dynamics	11
3.1	Hamiltonian and Equations of Motion	12
3.1.1	The Bohrian Coordinates	13
3.1.2	The Constants in \mathcal{L} and \mathcal{H}	14
3.2	Angular Momentum	14
3.2.1	Reduction of the Equations	15
4	Classical Chaos	17
4.1	Fundamentals	17
4.2	Lyapunov Exponent	19
5	Regularity and Lyapunov Exponent	21
5.1	Regularity	21
5.1.1	Error Estimation	27
5.2	Mean Leading Lyapunov Exponent	30
6	Treatise of the PAS	32
6.1	Kinematical Nature of the PAS	32
6.2	Relevance of the PAS for the Non-Rotating Case	33
6.3	Demonstrative Value of the PAS	34
6.3.1	Coordinate Degeneracy	35
6.3.2	Abrupt Changes and Avoided Crossings	35

7	Numerical Aspects	38
7.1	Determination of the Lyapunov Exponent	38
7.1.1	Method 1	39
7.1.2	Method 2	39
7.2	The Runge-Kutta Method	41
7.2.1	Basics	41
7.2.2	Error Estimation and Adaptive Stepsize Control	42
7.3	Estimation of Chaos Threshold	43
7.4	Computational Time	45
A	Constants of Motion and Integrability	46
A.1	The Non-rotating Case	46
A.2	The Rotating Case	47
B	Analysis of $J_{max}(E, B)$	49

Název práce: *Klasický chaos v geometrickém kolektivním modelu jader*

Autor: *Matúš Kurian*

Katedra (ústav): *Ústav teoretické fyziky*

Vedoucí diplomové práce: *Doc. RNDr. Pavel Cejnar, Dr.*

e-mail vedoucího: *cejnar@ipnp.troja.mff.cuni.cz*

Abstrakt: *Skúmame závislosť regularity systému s nenulovým momentom hybnosti na parametroch hamiltoniánu GCM pri nulovej energii. Zjednodušíme pôvodný hamiltonián využitím momentu hybnosti a získame jednoduchšie pohybové rovnice. Numericky určujeme regularitu systému pomocou hustoty stabilných trajektórií vo fázovom priestore. Počítame stredný hlavný Ljapunov exponent, všetko v rozsahu parametra $B \in [0, 0.5]$.*

Kľúčová slova: *Regularita systému, chaos, trajektória, Ljapunov exponent, GCM*

Title: *Classical Chaos in the GCM*

Author: *Matúš Kurian*

Department: *Institute of Theoretical Physics*

Supervisor: *Doc. RNDr. Pavel Cejnar, Dr.*

Supervisor's e-mail address: *cejnar@ipnp.troja.mff.cuni.cz*

Abstract: *We study behavior of regularity of the GCM in the case of non-zero angular momentum for zero energy. We show that the Hamiltonian can be simplified by using the angular momentum. We determine regularity of the system based on the density of stable trajectories in the phase space by numerical means. We also calculate the mean leading Lyapunov exponent, all of that for $B \in [0, 0.5]$.*

Keywords: *Regularity, chaos, trajectory, Lyapunov exponent, GCM*

Chapter 1

Introduction

Investigation of non-linear dynamics and chaos has become common in recent decades. The domain not only ceased to be an eccentric mathematical field of study as it had been in the age of H. Poincaré, but the progress in the theoretical department allowed numerous physicist to take part in it as well. Although their approach could sometimes be dubbed unrigorous, their focus is set firmly on the ever-expanding universe of chaotic phenomena.

The nuclear physics is no exception. Classical and quantum chaos has been being analyzed in many systems, and models. Despite the fact that such investigation might seem to lack practical application at times, it is invaluable to the understanding of the phenomenon. As chaos does exist in the nuclear physics, it would be most unwise to disregard it.

This work is an extension of thesis [1] that deals with the classical chaos in the geometric collective model. The model indeed exhibits chaotic behavior and possesses several interesting features. For these reasons, I believe that it was worth studying.

I decided to split this chapter into two parts. The first one presets an overview of the work. The other contains bibliographical notes on the chapter-by-chapter basis. Its purpose is to provide a clear insight into genesis of the work, so that the new material can be distinguished from the cited material.

1.1 Overview

One year ago Pavel Stránský presented and defended his thesis on classical chaos and phase transitions in the geometric collective model, [1]. He focused on a function of the system's regularity f_{reg} . This function – also termed *measure of regularity* was dependent on the parameters of the system. Now

the system was well described by the following Lagrangian:

$$\mathcal{L} = \frac{K}{2}(\dot{\beta}^2 + \beta^2\dot{\gamma}^2) - A\beta^2 - B\beta^3 \cos(3\gamma) - C\beta^4. \quad (1.1)$$

Such system would surely be integrable if $B = 0$.¹ Apparently, the cubic term can be regarded as a perturbation, and B as its strength.

The areal fraction of regular trajectories in a chosen Poincaré section was picked as a good measure of regularity.² Thus the dependence of f_{reg} on B was studied for zero energy. The result was a considerably complicated, non-monotonous function, see fig. 1.1, green line.

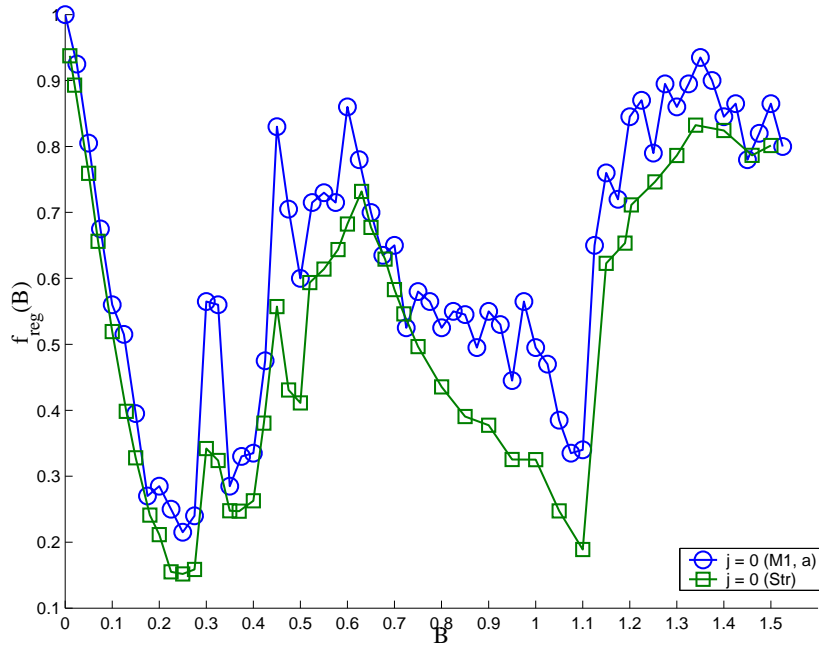


Figure 1.1: Dependence of regularity on B for the non-rotating case. green: results from [1] (fig. 4.2), blue: new results.

These results, however, were obtained for the non-rotating case. The influence of rotation on dependence (fig. 1.1) has not been studied.

This work attempts to fill the gap and address the question. The aforementioned rotation has to be understood as the mode of deformation that

¹See App. A.1.

²Chapter 5 is dedicated to explanation of the recurring words, such as regular, chaotic, stable.

has been so far suppressed.³

The classical angular momentum is the quantity that can be used for classification of possible cases.⁴ Firstly, its absence indicates absence of rotation. Secondly, j , the fraction of its instantaneous magnitude J and maximum magnitude J_{max} provides a notion of how much the system is rotating. Despite the more complicated nature of the rotating case, it can be shown⁵ that its Lagrangian is quite similar to (1.1):

$$\mathcal{L} = \frac{K}{2}(\dot{\beta}^2 + \beta^2\dot{\gamma}^2 + \beta^2\dot{\delta}^2 \sin^2\gamma) - A\beta^2 - B \cos(3\gamma)\beta^3 - C\beta^4. \quad (1.2)$$

The formal similarity of the Lagrangians does not automatically imply similarities in the f_{reg} . On the other hand, the limit of zero j (no angular momentum) must surely correspond to the old results (fig. 1.1). It can be safely concluded that this correspondence has been observed, see fig. 1.1, blue line.⁶

The method that has been employed by P. Stránský is based on the Poincaré sections. This approach was indeed viable and quite demonstrative, as the sections themselves provide a good picture of the system's behavior. This obvious advantage is based on the two-dimensional nature of the problem.⁷

The rotating case is essentially richer and more complicated. Its dimensionality is thus higher, cf. (1.2). Employment of the Poincaré sections is still possible, but they lose their greatest asset – demonstrative value. Even if we persisted, a direct comparison of these sections to the old ones would unlikely yield any worthwhile observations.

Once we decided to abandon the idea of Poincaré sections, a new method for measuring regularity of the system had to be proposed and established. A very natural criterion is the density of the regular (stable) trajectories in the phase space. For a very precise partition of the phase space this would be superior to the method of Stránský, as the *volume* density would be obtained – compared to the *surface* density of yore. Such construction is just purely theoretical because the computations are quite time-demanding, see sect. 7.4.

Stability of trajectories was tested by two alternative methods. One involves calculation of the leading Lyapunov exponent associated with the trajectory,

³More specific information concerning deformations and GCM can be found in Chapter 2.

⁴The angular momentum is properly defined by (3.8).

⁵Cf. sect. 3.2.1.

⁶Discrepancies in the correspondence will be discussed further in sect. 5.1.1.

⁷The dimensionality here refers to the number of degrees of freedom.

the other asymptotical properties, sect. 7.1. So the method of determining f_{reg} we employed is clearly different than in [1]. Therefore the correspondence of the lines in figure 1.1 provides a welcome proof that the method is valid and useful.

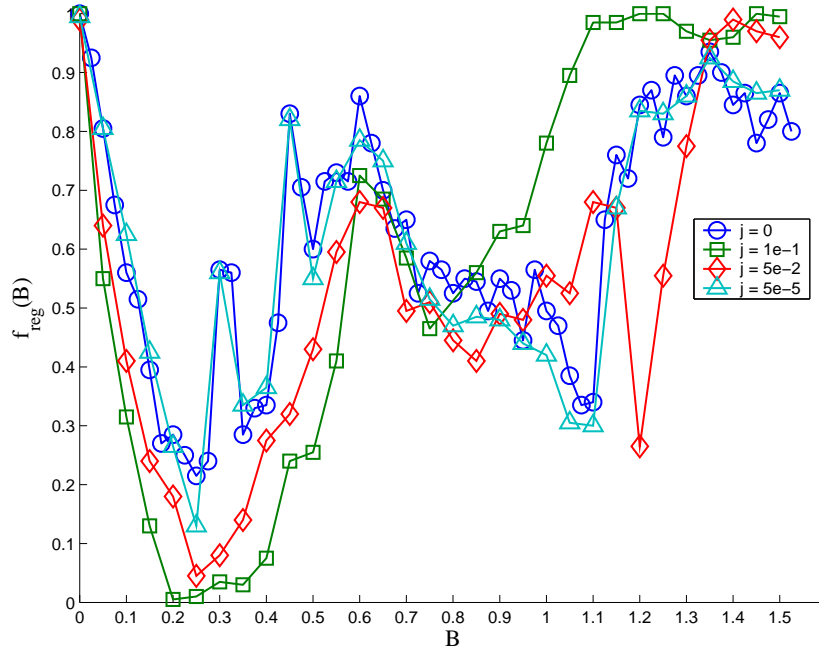


Figure 1.2: Dependence of the f_{reg} on B for four values of j .

Figure 1.2 shows that the presence of rotation *does change* the scenario. The essential general features of the results are visible here.⁸ The most prominent of them is existence of three distinct regions. The general behavior of f_{reg} is similar within a region, while it significantly differs from those from other regions. The following brief discussion will be made with reference to the zero level of angular momentum (blue line).

1. For $j \ll 0.05$ the graph approximates to the zero level of angular momentum.
2. For angular momenta $j \approx 0.05$ the picture resembles the non-rotating case in the middle of the interval. It copies the general behavior, but is much less accurate than the previous case.

⁸Chapter 5 contains more graphs and dedicated analysis. It also puts forward more precise estimates on bounds of regions 1-3. It also features analysis of error estimates.

3. For $j > 0.05$ the situation is considerably altered. The dependence falls into the first minimum, as it does rejoin on the top of $B \doteq 0.6$. It follows the referential line for a while, but breaks off at $B \doteq 0.75$ and the regularity is soon saturated.

A significant general trend is that *maximum regularity is attained for smaller values of B for increasing j* . Naturally more evidence is required and indeed shall be put forward later in Chapter 5.

Another standard quantity that is often studied in chaotic systems is the mean leading Lyapunov exponent σ .⁹ The preference of Poincaré sections in [1] means there are neither older results, nor a known limit reference point available. Our possibilities for comparison are limited as a consequence. Notwithstanding, a sample is given in fig. 1.3. We can safely state that the figure reaffirms the classification we have already introduced. Also, it can be said that the figure displays almost the same information in a different type of scale.

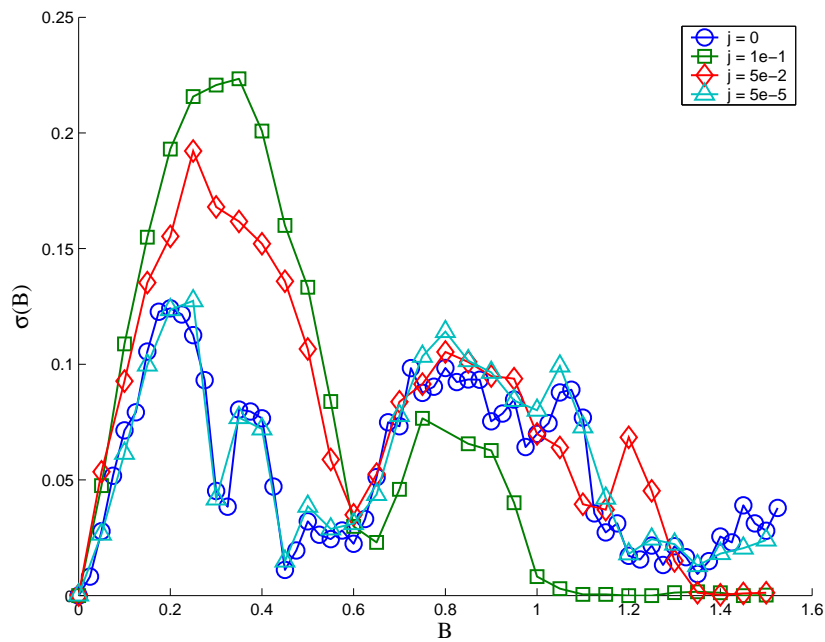


Figure 1.3: Dependence of the leading Lyapunov exp. σ on B for the same values of j .

⁹If the nomenclature seems awkward, refer to sect. 4.2.

1.2 Bibliographical Notes

Despite the fact that sources of information are nowadays properly cited, it is increasingly difficult to separate cited parts of the text from the original ones. The purpose of this section is to counter such unclarity by providing clearer grounds for a reader. The acquired important equations and concepts will be listed. The rest can be considered either as their derivatives or original work.

1. Introduction: It features the eq. (1.1) cited from [1].
2. Kinematics: the Chapter 2 draws heavily from [4]. In fact, there is little that could be added. The only slight innovation is an explicit introduction of the matrix α that has been taken from [1].
3. Dynamics: The origin of the starting equations is attributed to both [4] and [1]. The essential expressions (3.1) and (1.1) were taken from [1]. So were the expression for the angular momenta (3.8). The scaling of the Lagrangian (sec. 3.1.2), is attributed uniquely to [1]. The introduction of the Bohrian coordinates and simplification of the equations via J_3 are new concepts.
4. Classical Chaos: The concepts and definitions used there are more or less generally known. Little if any of what can found there is original.
5. Chapter Regularity and Lyapunov Exponent features figures, graphs and their analysis. Hardly anything could be attributed to other sources.
6. The Treatise of the PAS comprises expressions that are either original or those that have featured in the previous chapters. The name of the sec. 6.3.1 is a lease from [4].
7. Numerical Aspects: The part dealing with the RK is based entirely on the [8]. The recipe for use of *Method 2* was found directly at the website [3]. The other method has indeed been used in [2], but the implementation here is hardly more than inspired by the cited work, as it stems from the rather general concepts of the chaos theory.
8. The Appendices contain little of any bibliographical interest. The course of derivations, results, and possible errors are obviously original.

Chapter 2

The Kinematics of the GCM

2.1 Basics

The Geometric Collective Models has been proposed by Bohr and Mottelson ([9], [10]) and later elaborated by Faessler and Greiner ([11]). This work, however, does not focus on the model itself so the model will be presented in short. The book [4] is recommended as an excellent source of further information.

The GCM neglects the nuclear structure in favor of simplicity. The nucleus is considered a charged liquid drop. The surface layer is neglected as well. Precisely, we study deformations of the nuclear surface. These could be either rotations or vibrations.

The nuclear surface can be described by the following expansion:

$$R(\theta, \phi, t) = R_0 \left(1 + \sum_{\lambda=0}^{\infty} \sum_{\mu=-\lambda}^{\lambda} \alpha_{\lambda\mu}^*(t) Y_{\lambda\mu}(\theta, \phi) \right) \quad (2.1)$$

The α -s are known as the *shape parameters*. The parameters describe a change from the spherical configuration. As they are time-dependent they serve as *collective parameters*. Consequently, studying the nuclear motion turns into investigating the time-dependence of the collective parameters. The collective parameters possess the following noteworthy properties:¹

1. Complex conjugation:

$$\alpha_{\lambda\mu}^* = (-1)^\mu \alpha_{\lambda-\mu} \quad (2.2)$$

¹The simple proofs can be found in [4] and [1].

2. Transformation with respect to rotations:

$$\alpha'_{\lambda\mu} = \sum_{\mu'} \mathcal{D}_{\mu\mu'}^{(\lambda)} \alpha_{\lambda\mu'} \quad (2.3)$$

3. Transformation with respect to parity:

$$\alpha'_{\lambda\mu} = (-1)^\lambda \alpha_{\lambda\mu} \quad (2.4)$$

2.2 Quadrupole Deformations and the Principal Axes System

The expression (2.1) contains an infinite series. Eventually, it is possible to show that 0-th and 1-st order terms can be dropped, as they do not present proper deformations. Moreover, the series can be truncated, as the octupole and higher modes of deformation are negligible. (See [4] for details.) Now the eq. (2.1) becomes simpler:

$$R(\theta, \phi, t) = R_0 \left(1 + \sum_{\mu} \alpha_{2\mu}^*(t) Y_{2\mu}(\theta, \phi) \right) \quad (2.5)$$

So there are five complex collective parameters: $\{\alpha_{2-2}, \alpha_{2-1}, \alpha_{20}, \alpha_{21}, \alpha_{22}\}$. These, however are not independent, as a result of the (2.2). One can swiftly recognize that the parameters with negative second index are redundant. In addition, the α_{20} is real. In the end we conclude that there are five real parameters remaining: $\{\alpha_{21}^R, \alpha_{21}^I, \alpha_{20}, \alpha_{22}^R, \alpha_{22}^I\}$, where $\alpha_{2\mu} = \alpha_{2\mu}^R + i\alpha_{2\mu}^I$.

The collective parameters $\alpha_{2\mu}$ can also be termed as spherical. This corresponds to the fact that they arose via employment of the spherical coordinates. As ever, we are not bound to one set of coordinates. We will employ the cartesian coordinates now and demonstrate kinematical separation of rotation and vibration.

We begin with the expression analogous to the (2.1), where the expansion of the radius R would be done in (x, y, z, t) . The truncation of the series could be performed as well. As a result, the relevant collective parameters would be $\{\alpha_{xx}, \alpha_{xy}, \alpha_{yx}, \alpha_{yy}, \alpha_{yz}, \alpha_{zz}\}$. The relation between the spherical and cartesian

2.2 Quadrupole Deformations and the Principal Axes System 9

parameters are (cf. [1], [4]):

$$\begin{aligned}\alpha_{2\pm 2} &= \frac{1}{2}\sqrt{\frac{8\pi}{15}}(\alpha_{xx} - \alpha_{yy} \pm 2i\alpha_{xy}) \\ \alpha_{2\pm 1} &= \mp\sqrt{\frac{8\pi}{15}}(\alpha_{xz} \pm i\alpha_{yz}) \\ \alpha_{20} &= \sqrt{\frac{8\pi}{15}}\frac{1}{\sqrt{6}}(2\alpha_{zz} - \alpha_{xx} - \alpha_{yy})\end{aligned}\quad (2.6)$$

A few remarks should be made here. First, the cartesian parameters are real. Secondly, the subsidiary condition

$$\alpha_{xx} + \alpha_{yy} + \alpha_{zz} = 0$$

ensures the number of independent parameters totals five.

The cartesian parameters form the matrix of the second derivatives in the Taylor expansion (Hessian).² We rearrange the parameters into a matrix:³

$$\alpha = \begin{pmatrix} \alpha_{xx} & \alpha_{xy} & \alpha_{xz} \\ \alpha_{xy} & \alpha_{yy} & \alpha_{yz} \\ \alpha_{xz} & \alpha_{yz} & \alpha_{zz} \end{pmatrix}\quad (2.7)$$

Obviously, the matrix α is symmetric. So there exist such a basis that α becomes diagonal:

$$\alpha' = \begin{pmatrix} \alpha'_{xx} & 0 & 0 \\ 0 & \alpha'_{yy} & 0 \\ 0 & 0 & \alpha'_{zz} \end{pmatrix}\quad (2.8)$$

The trace of a matrix is invariant with respect to orthogonal coordinate transformations, so we safely assume there are only two independent parameters. And they *must* correspond to vibrations. This is apparent because (only) the rotations can be eliminated by a coordinate transformation.⁴

The special coordinate system is termed the *principal axes system* (PAS). Its choice is unique up to permutations of the axes and inversions.

It would appear that the PAS is the best system to describe the quadrupole

²This can be verified by a somewhat tedious explicit calculation that involves rewriting the spherical harmonics by cartesian coordinates. Unfortunately, both [1] and [4] contain the hint, but lack the proof itself.

³As it could have been observed earlier, we tacitly assume that partial derivatives of the radius with respect to coordinates commute.

⁴An arbitrary deformation of the continuum can be described by a sum of translation, rotation and proper deformation. Translation is not present in our case; it would be described by the first order in the expansion (2.1).

deformations. This is undoubtedly true whenever the deformations of the nucleus are reduced to vibrations.⁵ Its use for the more general case remains limited, though. (cf. Chapter 6)

2.2.1 The Bohr Coordinates

The equation (2.6) ensures that the only remaining spherical parameters in the PAS are α_{20} and α_{22} . Additionally, the latter is real, so we end up with α_{20} and α_{22}^R . As there are no other parameters left, we drop the superfluous indices:

$$\alpha_0 \equiv \alpha_{20}, \quad \alpha_2 \equiv \alpha_{22}^R.$$

A. N. Bohr proposed another set of coordinates in article [9]. They are essentially deformed polar coordinates in the plane (α_0, α_2) :

$$\begin{aligned} \alpha_0 &= \beta \cos \gamma, \\ \alpha_2 &= \frac{1}{\sqrt{2}} \beta \sin \gamma. \end{aligned} \tag{2.9}$$

The choice of the $\frac{1}{\sqrt{2}}$ is a shrewd one, as it guarantees that β^2 is invariant.⁶ Once a Lagrangian is constructed from α_0 and α_2 and their derivatives, it can be rewritten using the Bohr coordinates. Eventually, its form may be much simpler, cf. (1.1), (3.7).

⁵In this case the vibrations “stay in the primordial PAS.”

⁶Such β is a correct radial coordinate that remains constant under rotations cf. [9], [4].

Chapter 3

The Dynamics

Once the basic concepts, e.g. parameters of the model have been introduced, the dynamics can be investigated. This essentially comprises introduction of a Lagrangian or a Hamiltonian and derivation of the corresponding equations of motion. Finally, given certain constraints, both the Hamiltonian¹ and the equations can be simplified.

The first part of the chapter (sec. 3.1) follows chapter 2 of [1]. The construction of the Lagrangian, however, is not repeated here, so our starting point is the expression (2.25) in [1]. Immediately, we discard the terms including α_{21}^R , α_{21}^I and their derivatives. This will be justified in the later in the section 3.2.1. The constants in the Hamiltonian will be renamed as in [1], so we obtain the usual dependence on A , B , C and K . The last substitution will dispose of the multiplicative factors.

The penultimate section introduces Bohrian coordinates, while the last section summarizes the scaling properties of the Lagrangian. (cf. sec. 2.6 in[1])

The second part (sec. 3.2) deals with the angular momentum. We rewrite the appropriate expression that have been derived. Additionally, we have to give grounds for the simplification mentioned above, so the rest of the section will be dedicated to this end.

¹The Hamiltonian formalism is slightly preferred in this work, but the same simplification could be done in the Lagrangian. In the course of the chapter both the Lagrangian and Hamiltonian are used.

3.1 Hamiltonian and Equations of Motion

The Lagrangian that has been put forward in [1] is:

$$\begin{aligned}
\mathcal{L} = & + \frac{B_2}{\sqrt{5}} (|\dot{\alpha}_{20}|^2 + 2|\dot{\alpha}_{21}|^2 + 2|\dot{\alpha}_{22}|^2) - \\
& - \frac{C_2}{\sqrt{5}} (|\alpha_{20}|^2 + 2|\alpha_{21}|^2 + 2|\alpha_{22}|^2) - \\
& - C_3 \sqrt{\frac{2}{35}} \left\{ \alpha_{20} (-|\alpha_{20}|^2 - 3|\alpha_{21}|^2 + 6|\alpha_{22}|^2) - \right. \\
& \left. - 3\sqrt{6} [\alpha_{22}^R (\alpha_{21}^R \alpha_{21}^R - \alpha_{21}^I \alpha_{21}^I) + 2\alpha_{22}^I \alpha_{21}^R \alpha_{21}^I] \right\} - \\
& - \frac{C_4}{5} (|\alpha_{20}|^2 + 2|\alpha_{21}|^2 + |\alpha_{22}|^2)^2. \tag{3.1}
\end{aligned}$$

Following the cited work, the constants A , B , C , and K are introduced:

$$K \equiv \frac{2B_2}{\sqrt{5}}, \quad A \equiv \frac{2C_2}{\sqrt{5}}, \quad B \equiv -C_3 \sqrt{\frac{2}{35}}, \quad C \equiv \frac{C_4}{5}. \tag{3.2}$$

Moreover, we will use the fact the following statement:

$$\dot{\alpha}_{21}^R(t) = 0 \quad \& \quad \dot{\alpha}_{21}^I(t) = 0 \quad \forall t.$$

Its proof requires the form of the angular momentum that has not been introduced yet, so it has to be postponed to the section 3.2.1. Additionally it carries some formal restrictions as well.

Immediately, the following substitution can be proposed:

$$\eta \equiv \alpha_{20}, \quad \xi \equiv \sqrt{2}\alpha_{22}^R, \quad \zeta \equiv \sqrt{2}\alpha_{22}^I.$$

The Lagrangian now becomes simpler – the multiplicative factors of 2 have been eliminated.²

$$\mathcal{L} = \frac{K}{2} (\dot{\eta}^2 + \dot{\xi}^2 + \dot{\zeta}^2) - A(\eta^2 + \xi^2 + \zeta^2) + B\eta[3(\xi^2 + \zeta^2) - \eta^2] - C(\eta^2 + \xi^2 + \zeta^2)^2 \tag{3.3}$$

The Hamiltonian is then:

$$\mathcal{H} = \frac{1}{2K} (\pi_\eta^2 + \pi_\xi^2 + \pi_\zeta^2) + A(\eta^2 + \xi^2 + \zeta^2) - B\eta[3(\xi^2 + \zeta^2) - \eta^2] + C(\eta^2 + \xi^2 + \zeta^2)^2, \tag{3.4}$$

²A note of caution is needed: These new coordinates are not the ones employed by Greiner in section 6.2.3 of [2]

where the generalized momenta are defined by:

$$\pi_\eta \equiv \frac{\partial \mathcal{L}}{\partial \dot{\eta}} = K\dot{\eta}, \quad \pi_\xi \equiv K\dot{\xi}, \quad \pi_\zeta \equiv K\dot{\zeta}.$$

So we arrive to following canonical equations of motion:

$$\begin{aligned} \dot{\eta} &= \frac{1}{K} \pi_\eta \\ \dot{\pi}_\eta &= -2A\eta + 3B(\xi^2 + \zeta^2 - \eta^2) - 4C\eta(\eta^2 + \xi^2 + \zeta^2) \\ \dot{\xi} &= \frac{1}{K} \pi_\xi \\ \dot{\pi}_\xi &= -2\xi[2A - 3B\eta + 2C(\eta^2 + \xi^2 + \zeta^2)] \\ \dot{\zeta} &= \frac{1}{K} \pi_\zeta \\ \dot{\pi}_\zeta &= -2\zeta[2A - 3B\eta + 2C(\eta^2 + \xi^2 + \zeta^2)] \end{aligned} \quad (3.5)$$

It is remarkable that the equations for ξ and ζ are related by the transformation $\xi \leftrightarrow \zeta$. This could have already been anticipated from the form of the Hamiltonian (3.4).

Due to the technical its nature discussion of the integrals of motion and integrability of the Lagrangian (3.3) is postponed to the Appendix A.

3.1.1 The Bohrian Coordinates

The paragraph presents Bohrian³ coordinates. They stem from the form of (3.3) and the original Bohr coordinates (2.9). Effectively they are spherical coordinates:⁴

$$\begin{aligned} \xi &= \beta \sin \gamma \sin \delta, & \beta &\in (0, \infty) \\ \zeta &= \beta \sin \gamma \cos \delta, & \gamma &\in [0, \pi) \\ \eta &= \beta \cos \gamma, & \delta &\in [0, 2\pi). \end{aligned} \quad (3.6)$$

The Lagrangian (3.3) can be easily recast:

$$\mathcal{L} = \frac{K}{2}(\dot{\beta}^2 + \beta^2\dot{\gamma}^2 + \beta^2\dot{\delta}^2 \sin^2 \gamma) - A\beta^2 - B \cos(3\gamma)\beta^3 - C\beta^4. \quad (3.7)$$

³A new set of coordinates inspired by the Bohr one. The name distinguishes them from the proper Bohr coordinates (cf. 2.9) while preserving their origin.

⁴Note that they are spherical with respect to the *rescaled* parameters (ξ, ζ, η) . The expressions would include factors $\frac{1}{\sqrt{2}}$ if $(\alpha_{22}^R, \alpha_{22}^I, \alpha_{20})$ were on the right-hand-side of the (3.6). Eventually refer to (2.9).

This form of the Lagrangian is suitable for further calculations, as the potential is *the same* as in the case with zero angular momentum. The corresponding Hamiltonian and equations of motion can be derived straightforwardly, and therefore we omit them.

3.1.2 The Constants in \mathcal{L} and \mathcal{H}

Both the expression (3.4) and (3.7) contain four unspecified constants A , B , C , and K . Despite that the Lagrangian can be considered one-parametric. This is enabled by the scaling of the equations described in the section 2.6 of [1]. Here, it suffices to say we adapt the parametrization by B . The remaining parameters shall be set as follows:

$$-A = C = K = 1.$$

Not only will this approach lead to easy comparison of the results with those published in [1], but it is natural as well. The B can be identified as the strength of perturbation.⁵

3.2 Angular Momentum

In the section 2.2.1 of [1] the author has constructed the angular momentum appropriate for the system using the tensor operators.

$$\begin{aligned} J_1 &= 2\sqrt{\frac{2}{5}} B_2 \left[\sqrt{2}(\alpha_{21}^I \dot{\alpha}_{22}^R - \dot{\alpha}_{21}^I \alpha_{22}^R + \dot{\alpha}_{21}^R \alpha_{22}^I - \alpha_{21}^R \dot{\alpha}_{22}^I) + \sqrt{3}(\dot{\alpha}_{20} \alpha_{21}^I - \alpha_{20} \dot{\alpha}_{21}^I) \right] \\ J_2 &= -2\sqrt{\frac{2}{5}} B_2 \left[\sqrt{2}(\dot{\alpha}_{21}^R \alpha_{22}^R - \alpha_{21}^R \dot{\alpha}_{22}^R + \dot{\alpha}_{21}^I \alpha_{22}^I - \alpha_{21}^I \dot{\alpha}_{22}^I) + \sqrt{3}(\dot{\alpha}_{20} \alpha_{21}^R - \alpha_{20} \dot{\alpha}_{21}^R) \right] \\ J_3 &= \frac{4}{\sqrt{5}} B_2 [\dot{\alpha}_{21}^R \alpha_{21}^I - \alpha_{21}^R \dot{\alpha}_{21}^I + 2(\dot{\alpha}_{22}^R \alpha_{22}^I - \alpha_{22}^R \dot{\alpha}_{22}^I)] \end{aligned}$$

Once B_2 is substituted by K (3.2) we obtain:

$$\begin{aligned} J_1 &= \sqrt{2}K \left[\sqrt{2}(\alpha_{21}^I \dot{\alpha}_{22}^R - \dot{\alpha}_{21}^I \alpha_{22}^R + \dot{\alpha}_{21}^R \alpha_{22}^I - \alpha_{21}^R \dot{\alpha}_{22}^I) + \sqrt{3}(\dot{\alpha}_{20} \alpha_{21}^I - \alpha_{20} \dot{\alpha}_{21}^I) \right] \\ J_2 &= \sqrt{2}K \left[\sqrt{2}(\dot{\alpha}_{21}^R \alpha_{22}^R - \alpha_{21}^R \dot{\alpha}_{22}^R + \dot{\alpha}_{21}^I \alpha_{22}^I - \alpha_{21}^I \dot{\alpha}_{22}^I) + \sqrt{3}(\dot{\alpha}_{20} \alpha_{21}^R - \alpha_{20} \dot{\alpha}_{21}^R) \right] \\ J_3 &= 2K [\dot{\alpha}_{21}^R \alpha_{21}^I - \alpha_{21}^R \dot{\alpha}_{21}^I + 2(\dot{\alpha}_{22}^R \alpha_{22}^I - \alpha_{22}^R \dot{\alpha}_{22}^I)] \end{aligned} \quad (3.8)$$

The three components of the angular momentum constitute three integrals of motion. This stems from the way they have been derived, cf. section 2.2.1 in [1]. Alternatively the statement can be verified by explicit

⁵The system described by (3.7) is integrable when $B = 0$, see also app. A.2.

calculation.

Note, however that these integrals of motion are *not* in involution, as the corresponding Poisson brackets do not vanish. So there exist only three independent and compatible constants of motion: energy, one component of the angular momentum⁶ and the total angular momentum. We have to deal with five degrees of freedom, so we can expect that the system will not be fully integrable.⁷

Last, discussion of maximal angular momenta for a given energy and parameter B can be found in appendix B.

3.2.1 Reduction of the Equations

Assume, the system contains an arbitrary angular momentum \vec{J} , $\vec{J} = (J_1, J_2, J_3)$. There is no doubt, however that it is possible to choose a coordinate system so that $\vec{J} = (0, 0, |\vec{J}|)$, if $\vec{J} \neq \vec{0}$.⁸ Now the most general case when $J_1 = J_2 = 0$ and $J_3 = J \neq 0$ implies

$$\alpha_{21}^R = \dot{\alpha}_{21}^R = \alpha_{21}^I = \dot{\alpha}_{21}^I = 0.$$

Proof: The statement follows from the form of (3.8):

$$\begin{aligned} J_1 &= \sqrt{2}K \left[\sqrt{2}(\alpha_{21}^I \dot{\alpha}_{22}^R - \dot{\alpha}_{21}^I \alpha_{22}^R + \dot{\alpha}_{21}^R \alpha_{22}^I - \alpha_{21}^R \dot{\alpha}_{22}^I) + \sqrt{3}(\dot{\alpha}_{20} \alpha_{21}^I - \alpha_{20} \dot{\alpha}_{21}^I) \right] = 0, \\ J_2 &= \sqrt{2}K \left[\sqrt{2}(\dot{\alpha}_{21}^R \alpha_{22}^R - \alpha_{21}^R \dot{\alpha}_{22}^R + \dot{\alpha}_{21}^I \alpha_{22}^I - \alpha_{21}^I \dot{\alpha}_{22}^I) + \sqrt{3}(\dot{\alpha}_{20} \alpha_{21}^R - \alpha_{20} \dot{\alpha}_{21}^R) \right] = 0. \end{aligned}$$

So the expression for $\frac{J_1 \pm J_2}{\sqrt{2}K}$ is equal to:

$$\begin{aligned} \frac{J_1 \pm J_2}{\sqrt{2}K} &= \sqrt{2}\alpha_{22}^R(\dot{\alpha}_{21}^R \mp \dot{\alpha}_{21}^I) + \sqrt{2}\dot{\alpha}_{22}^R(\alpha_{21}^I \mp \alpha_{21}^R) + \sqrt{2}\alpha_{22}^I(\dot{\alpha}_{21}^R \pm \dot{\alpha}_{21}^I) - \\ &\quad - \sqrt{2}\dot{\alpha}_{22}^I(\alpha_{21}^R \pm \alpha_{21}^I) + \sqrt{3}\dot{\alpha}_{20}(\alpha_{21}^I \pm \alpha_{21}^R) - \sqrt{3}\alpha_{20}(\dot{\alpha}_{21}^I \pm \dot{\alpha}_{21}^R) = 0. \end{aligned}$$

If we require that α_{20} , α_{22}^R , α_{22}^I and $\dot{\alpha}_{20}$, $\dot{\alpha}_{22}^R$, $\dot{\alpha}_{22}^I$ are independent and arbitrary, then the equation holds only if the terms in the parentheses are zero. This, however is only possible if both terms in the parentheses are zero. It follows that $\alpha_{21}^R = \dot{\alpha}_{21}^R = \alpha_{21}^I = \dot{\alpha}_{21}^I = 0$. We briefly check that J_3 can be still non-zero in these circumstances. As it can, the proof is complete. ■

Now, we can apply the parametrization by (η, ξ, ζ) and obtain the Hamiltonian in the form (3.4). The simplification is a considerable asset, as the

⁶The third component tends to be preferred, and so it will be in our case

⁷See app. A for details.

⁸Otherwise the problem becomes very simple indeed, cf. section 2.2.2 in [1].

number of equations that have to be solved has been decreased. The computational time will be reduced as well.⁹

The resulting case is 3-D. However, the system is still not integrable. There are only two independent and compatible integrals of motion at our disposal, because the norm of the angular momentum is now dependent on J_3 . In fact, $|\vec{J}| = |J_3|$, as we designed.

⁹The issue of computation time is indeed relevant, see section 7.4.

Chapter 4

Classical Chaos

The chapter summarizes basic concepts of the chaos theory. It is not meant as an extensive overview; it rather provides definitions of the concepts that are frequently used. There is no standard recommended reference book to this chapter. The voluminous [7] could surely be used, but it is unnecessary. The chaos theory is usually based on the Hamiltonian formalism, so a few definitions will be repeated for convenience.

4.1 Fundamentals

A system with N degrees of freedom is described by N *generalized coordinates* q_i and N *generalized momenta* p_i . The corresponding $2N$ -dimensional Euclidean space is referred to as the *phase space*.

All quantities in the Hamiltonian mechanics are functions of the coordinates, momenta and time.

The center of the Hamiltonian mechanics is the Hamilton function or Hamiltonian, $\mathcal{H}(q, \pi, t)$. The Hamiltonian equation of motions have the following shape:

$$\dot{q}_k = \frac{\partial \mathcal{H}}{\partial \pi_k}, \quad (4.1a)$$

$$\dot{\pi}_k = -\frac{\partial \mathcal{H}}{\partial q_k}. \quad (4.1b)$$

A solution of the equation of motions is termed as a *trajectory*. Note that trajectory also contains velocities, so it comprises more information than a photography.

An important concept of the Hamiltonian mechanics is the Poisson bracket.

Definition: *The Poisson bracket*

If A and B are functions of canonical coordinates and momenta, then their Poisson bracket is defined by

$$\{A, B\}_{\text{Poiss}} = \sum_{i=1}^N \left(\frac{\partial A}{\partial q_i} \frac{\partial B}{\partial \pi_i} - \frac{\partial A}{\partial \pi_i} \frac{\partial B}{\partial q_i} \right), \quad (4.2)$$

where N is equal to the number of degrees of freedom.

The Poisson bracket possess a number of well-known properties: antisymmetry in arguments, linearity in both arguments. Jacobi identity also holds for a Poisson bracket.

An integral of motion is a quantity that is preserved:

Definition: *An Integral of Motion*

$Q(q, \pi)$ is an integral of motion $\Leftrightarrow \frac{dQ}{dt} = 0$.

Alternatively we can make the **Statement:**

$Q(q, \pi, t)$ is an integral of motion $\Leftrightarrow \{Q, H\}_{\text{Poiss}} = 0$.

The proof of is a standard issue of the theoretical mechanics.

Definition: *Compatibility*

J and K are compatible only if their Poisson bracket vanishes.

A set is said to contain compatible quantities if they are pairwise compatible.

Now we are able to restate the last **Statement:**

The integrals of motion are quantities that are compatible with the Hamiltonian.

Definition: *An Integrable System*

A system is integrable only if it possesses a set of N independent and compatible integrals of motion.

It follows that systems which possess fewer constants of motion are non-integrable or *chaotic*.

Now that we have defined integrability, we can prove that the systems defined by Lagrangians (1.1) and (1.2) are integrable in the special case $B = 0$, see Appendix A.

4.2 Lyapunov Exponent

The Lyapunov exponent is very useful concept describing separation of close trajectories in the phase space.

Suppose we have a trajectory, $z(t) = [q(t), p(t)]$. Consider another one, $\tilde{z}(t)$ initially very close to the first one:

$$\tilde{z}(t) - z(t) = \delta(t), \quad \delta(0) = \varepsilon \hat{\delta}_0, \quad |\hat{\delta}_0| = 1, \quad \varepsilon \in \mathbb{R}.$$

Definition: *Rate of Divergence*

$$\text{Let } R(t) \equiv \frac{|\delta(t)|}{|\delta(0)|} \quad \text{so in our case: } R(t) = \frac{|\delta(t)|}{\varepsilon}.$$

The time-evolution of $R(t)$ is crucial. We usually study dependence of $\ln R(t)$, however. Let us define the limit:

Definition: *Leading Lyapunov Exponent*

$$\sigma \equiv \lim_{t \rightarrow \infty} \frac{\ln R(t)}{t}. \quad (4.3)$$

Note: Sometimes one might encounter “mean” or “average” (leading) Lyapunov exponents. This usually suggests space averaging.

The last notion allows us to distinguish regular¹ and chaotic trajectories by virtue of the following definition.²

Definition: *Stability*

Whenever the leading Lyapunov exponent of a trajectory is zero, it is termed *regular* or *stable*. Otherwise it is *unstable* or *chaotic*.

Note: There are no chaotic trajectories in an integrable system. Integrability implies (full) regularity.

Definition: *Measure of Regularity*

In general a measure function that measures a regularity-related quantity is a measure of regularity.

We are more specific – volume density of initial conditions corresponding to stable trajectories is considered to be *the* measure of regularity.

¹This word will be used in two different ways. Stable trajectories will be sometimes termed regular. And we will say the system is more/less regular depending on its measure of regularity.

²A mathematical purist would surely be justly enraged about the use of definition for such a cause, but we have not introduced enough concepts to make a proper statement.

It would seem that everything is well-defined. The definition (4.3) is a bit problematic, though. It has to be amended for cases of *bounded* systems that do not support infinite divergence of trajectories. Despite the fact that this is of real concern, we will not pursue it formally any further. Rather, we hope to propose criteria for stability of trajectories on the *operational basis*. This process is described in detail in section 7.1.

Chapter 5

Regularity and Lyapunov Exponent

The chapter presents results of numerical computations and their subsequent analysis. We studied both the dependence of regularity (f_{reg}) and mean leading Lyapunov exponent (σ) on j . In order to have done that, the equations of motion (3.5) had to be solved.¹ Whenever it was possible, 200 trajectories² were chosen for a pair (j, B) . This should ensure that results are not taxed heavily by randomness.

The chapter is divided into two parts. The first one aims on regularity and the other on the mean leading Lyapunov exponent. As the topic of the regularity stems from [1], it will be slightly preferred. The discussion of the figures will be complemented with error estimation.

The Lyapunov section will be briefer, as there is no such need for a lengthy scrutiny.

5.1 Regularity

Investigation of the regularity was our primary objective. We wanted to compute regularity for the rotating case and analyze it. Last, we intended to compare to the results with those published in [1].

Let us recall that the density of the regular trajectories is taken as a measure of regularity. This density was studied as a function of B for various values of j . The energy of the system was kept zero in all cases.

¹The Chapter 7 lists methods, tricks, their advantages, vices and loopholes.

²The graphs for $j \leq 10^{-4}$ and the red line in fig. 5.6 used fewer initial conditions. The red line took its time, see sec. 7.4. Generation of the initial conditions proved time and space consuming for very small j -s.

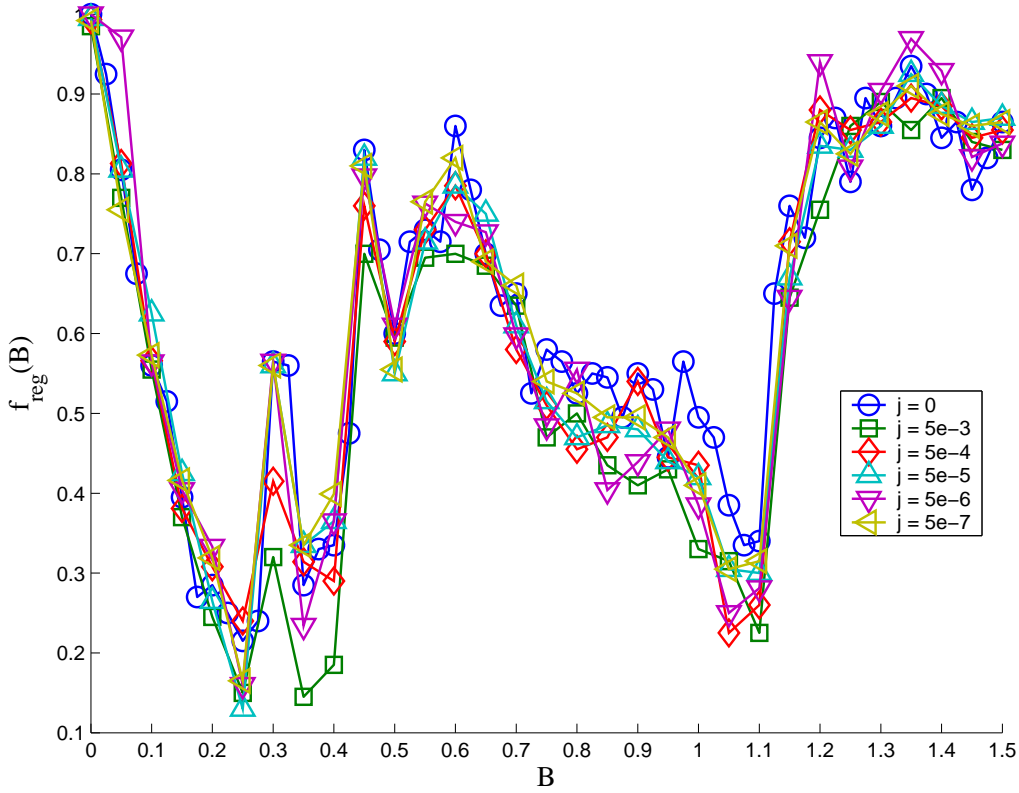


Figure 5.1: Regularity in the region of small j .

The simulations show that the dependence of f_{reg} on j is non-random. In fact, it shows reasonable behavior. This justifies the choice of j as the classification parameter *ex postfacto*.

The j -dependence of the f_{reg} is best characterized by description of the following regions:

1. Region of small j -s, $j \in [0, 0.005]$

The dependence of regularity in this region copies very much the canonical dependence of the non-rotating case. This is demonstrated in fig. 5.1. The graphs of regularity exhibit the same pattern and tend to follow one another.

The graph of $f_{\text{reg}}^{j=0}$ has the following extrema: three prominent local maxima $B = \{0.3, 0.45, 0.6\}$ and four local minima $B = \{0.25, 0.35, 0.5, 1.1\}$. Additionally, there is a highly regular, though not a saturated tail from $B \geq 1.3$.

Yet, there is a suggestion of a decreasing trend at the first peak ($B =$

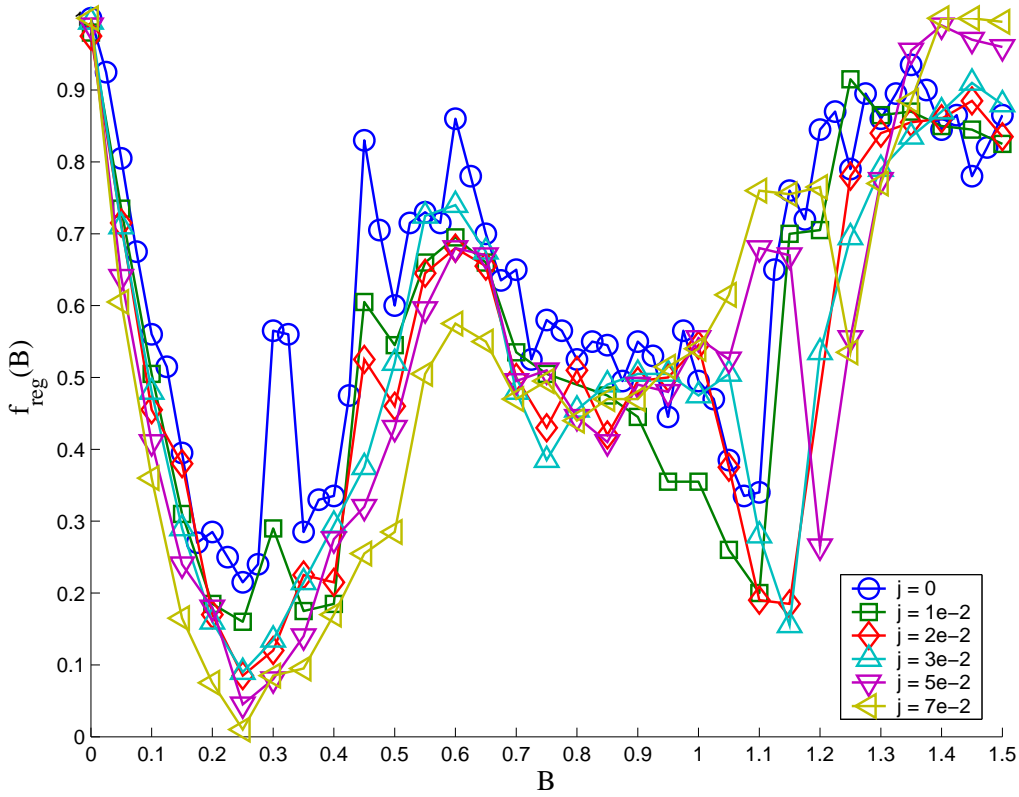


Figure 5.2: $f_{\text{reg}}(B)$ in the transition region.

0.3), where the graphs for lower j tend to go higher than their more rotating counterparts. This tendency continues even in the transition region and well beyond it. So we conclude that this local peak gradually vanishes with increasing j .

2. Transition³ region, $j \approx 0.01$

The general features of the dependence start to alter subtly here. The minimum at $B \doteq 1.1$ moves towards greater B -s and becomes shallower. At the same time, the descending monotonous part $[0.65, 1.1]$ starts to level. This can be observed well on the height of the peak at $B \doteq 0.6$. This is shown in fig. 5.2, and fig. 5.3.

Figure 5.2 depicts all instances that have been computed in the region, along with the referential $f_{\text{reg}}^{j=0}$. For greater convenience a selection is

³The name suggests resemblance to the previous case, while also inducing an idea of progressing changes.

provided in figure 5.3. The transitional character of the region becomes more evident there.

The drift of the deep minimum and its eventual rise can be observed well. Moreover, the monotonous character of the interval $[0.65, 1.1]$ is changed. Eventually there is an important rising trend at the end of the interval for both $j = 0.05$, and $j = 0.07$.

Another interesting observation is that

$$f_{\text{reg}}^{j=0} \geq f_{\text{reg}}^{j=0.03} \geq f_{\text{reg}}^{j=0.05} \geq f_{\text{reg}}^{j=0.07}$$

on the interval $[0.0, 0.65]$. And we note that maxima of $f_{\text{reg}}^{j=0}$ are not followed closely any longer at $B = \{0.3, 0.45\}$ at all. At $B = 0.6$ the correspondence is not much greater in absolute numbers, but the extremal character of the point is preserved. Eventually, this is one of the few features that are (partly) retained in the last region.

3. Post-transitional region, $j \geq 0.1$

This region ceases to possess resemblance to the previous ones. We note that the first local minimum is a bit deeper and much broader: regularity becomes zero on a “seabed” (approx. $B \in [0.15, 0.35]$) for all species. Afterwards, the general trend is a sharp rise to the maximal regularity. So the first part of f_{reg} comes in the shape of U, while the second is plain constant. The graph of $f_{\text{reg}}^{j=0.1}$ differs from the others a bit. It does not feature the simple U-and-constant shape, and it sticks to $f_{\text{reg}}^{j=0}$ between 0.65 and 0.80. Actually this makes it rather similar to the case $f_{\text{reg}}^{j=0.07}$ from fig 5.3. Apparently, the two display some similar properties. On the other hand, the $f_{\text{reg}}^{j=0.07}$ has a shallow minimum at $B = 1.25$ that stamps the region of low and middle j -s. The graph of $f_{\text{reg}}^{j=0.1}$ seems to have lost it. As a result, this particular case was sorted to the post-transitional region.

Generally, we can state that the saturation of regularity shifts towards smaller B -s with increasing j . Otherwise said, the presence of significant angular momentum tends to *stabilize* the system. It has not been observed that its presence has detrimental effects on regularity in the domain.

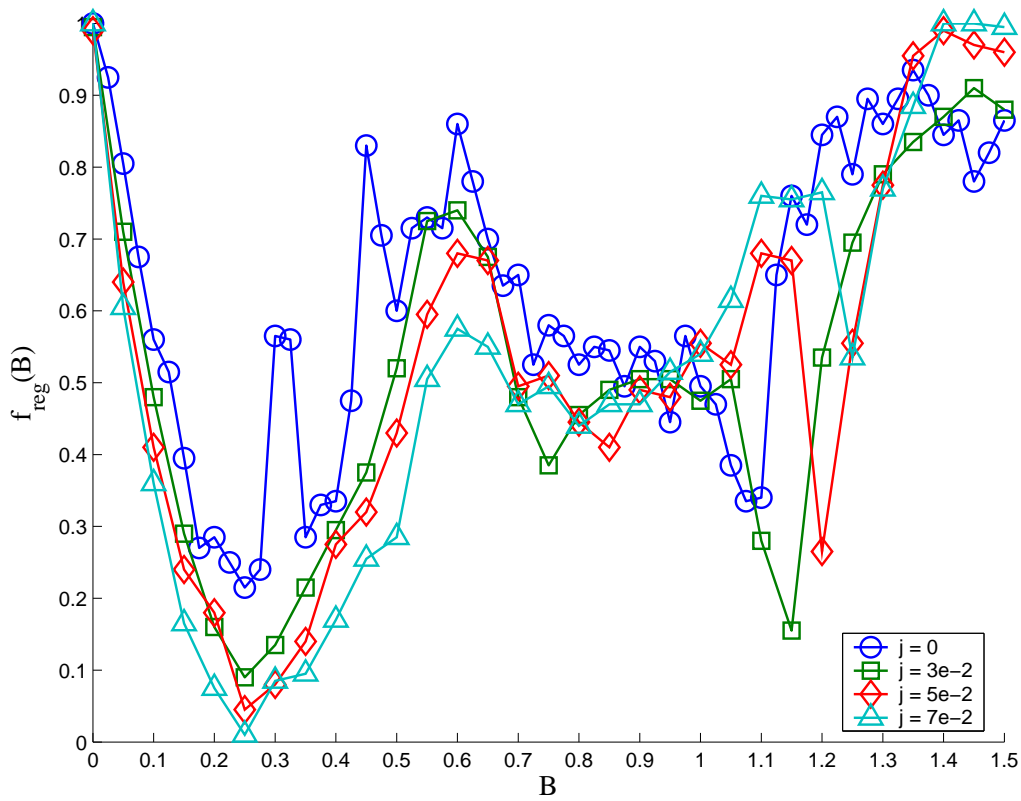


Figure 5.3: A selection in the transition region – The deep minimum shifts towards greater B -s gets shallower. The descending part $[0.65, 1.1]$ is becoming more level.

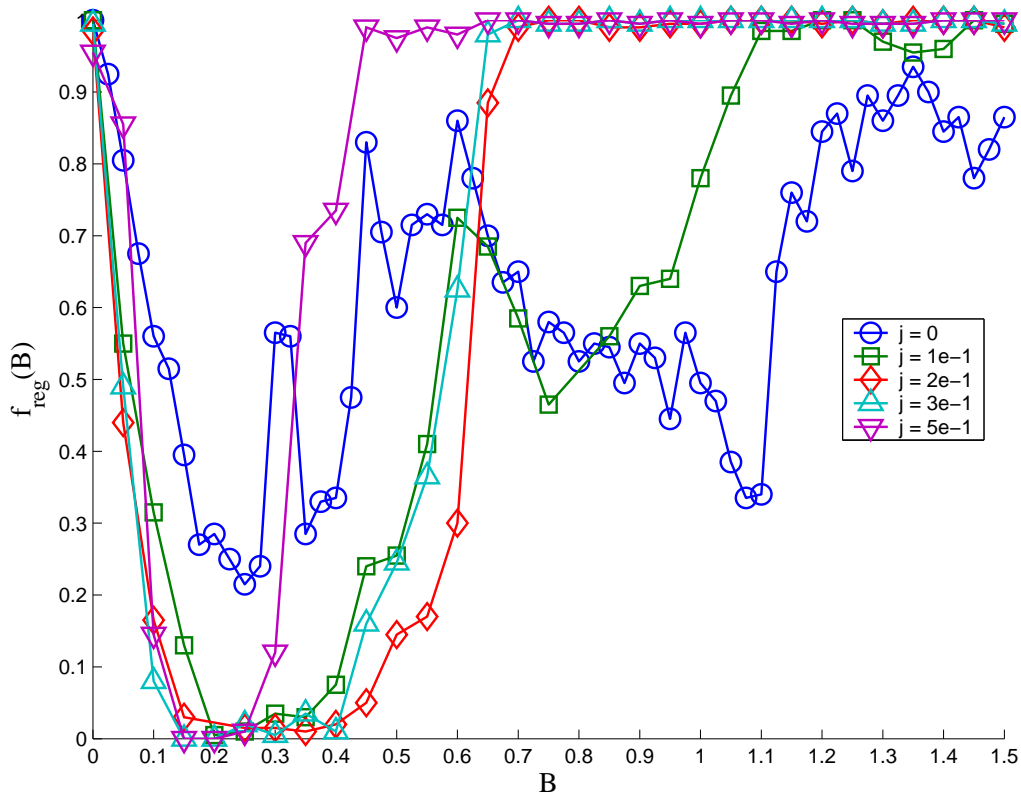


Figure 5.4: Post-translational region – the scenario changed dramatically. Note the two distinct parts of the f_{reg} : the U-part and the constant part.

5.1.1 Error Estimation

There is a notion that a statistical error associated with randomness might play a role here. The randomness arises mainly from generation of the initial conditions and their perturbations. The existence of such source of error can be tested by a repetition of the calculation for the same j . Figure 5.5 depicts

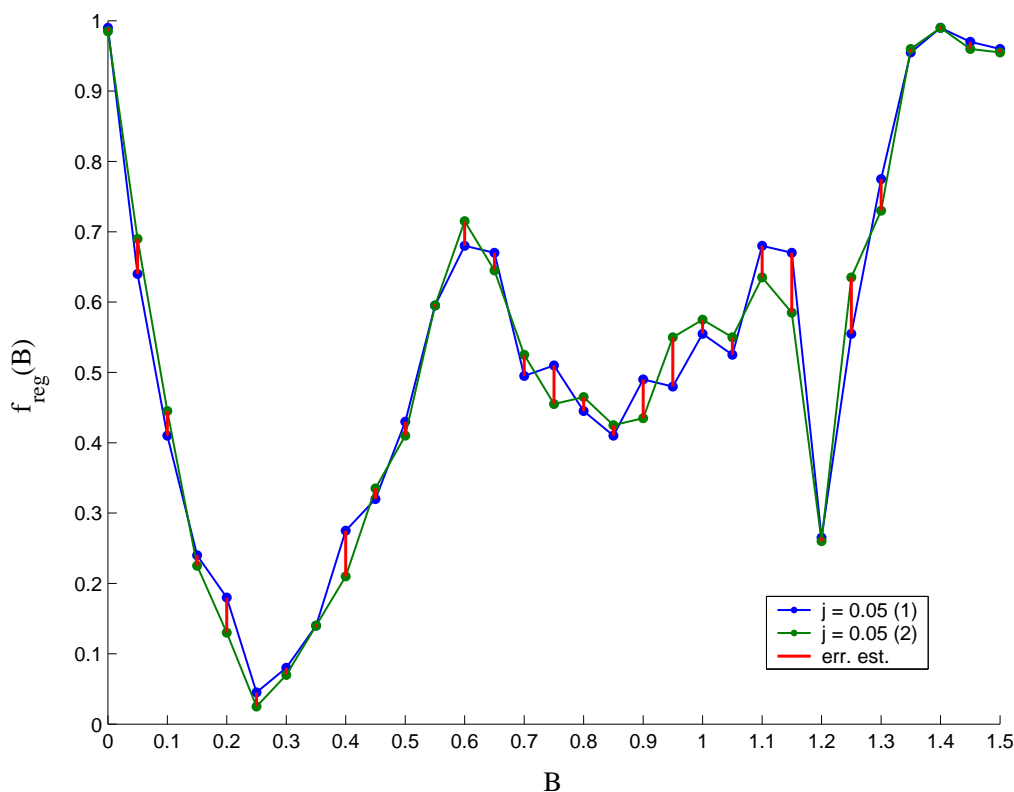


Figure 5.5: Estimation of statistical error.

such an attempt. The maximal absolute difference between the two sets is $\Delta = 0.085$. The value of the estimate is not terribly surprising, although it is far from negligible. Still, the flawed correspondence in fig. 1.1 should lead our path. As the estimate of the statistical error is not big enough to explain the discrepancy, we have to search further.

We might assume that our method is not free of systematic errors.⁴ These have to be tackled in a more subtle way. We might use comparison between the “old” and “new” results of f_{reg} for the non-rotating case. Let us collect

⁴It would be quite unwise to presume the opposite.

all results for $j = 0$ that we have at our disposal along with the technical information concerning those methods. (fig. 5.6)

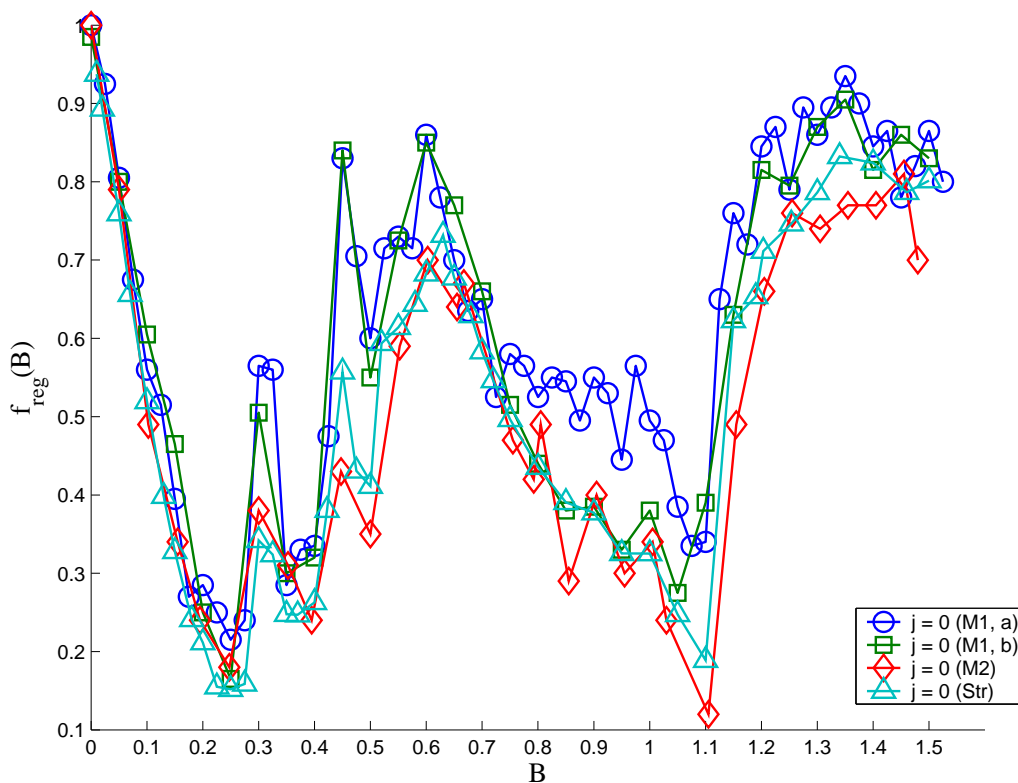


Figure 5.6: Estimation of systematic error.

- i) Blue line: The standardly-used f_{reg} dependence. We used Method 1 from sect. 7.1 for calculations. The maximal amplitude of the random generator was default.
- ii) Green line: Method 1 was used as well, but the maximal amplitude of the generator was enlarged.
- iii) Red line: The Method 2 was employed, and the amplitude of the generator should be around default.
- iv) Cyan line: The result from [1], based on the Poincaré sections.

Let us assume that the cyan line is the least erroneous. Additionally, suppose that the areal approach is close to the volume approach, e.i. that

the system does not exhibit exotic properties on the Poincaré section. Now this assumption may not seem as plausible as the previous one. However, note that the cyan line is bounded most of the time by the red and the green ones. So no matter what devilry might lurk there, the state of the Poincaré section is quite close to the state of the whole system.

We know⁵ that the Method 2 contains parameter $\sigma_{\text{threshold}}$. This parameter is most critical for correct distinction between regular and chaotic trajectories, so it could act an exceptionally efficient generator of systematic errors. So we might suspect that its existence undermines reliability of the method. However, it is evident that this method is generally more precise, so we should not be making hasty decisions.

There is a similar problem even in the Method 1 – the intermediate trajectories. These could be mistaken for regular trajectories. Such lapse would indeed induce a systematic error that would *increase* regularity. So is the density of intermediate trajectories significantly higher than normal at $B = 0.3$ and $B = 0.5$ for $j = 0$? Or is the assumption about greater validity of older results vain? We do not know.

Given the information we have, the questions about the discrepancy remains unresolved. And a decent systematic error estimate for Method 1 climbs up to 0.17 while disregarding the extrema. ($B = 0.3$ and $B = 0.5$)

⁵Cf. sect. 7.1.

5.2 Mean Leading Lyapunov Exponent

The dependence of the leading Lyapunov exponent will be presented, but not commented extensively. The division of the regions is left unchanged. There is no special figure for the zero-level dependence, though. As it was explained a need for such figure is considerably smaller.

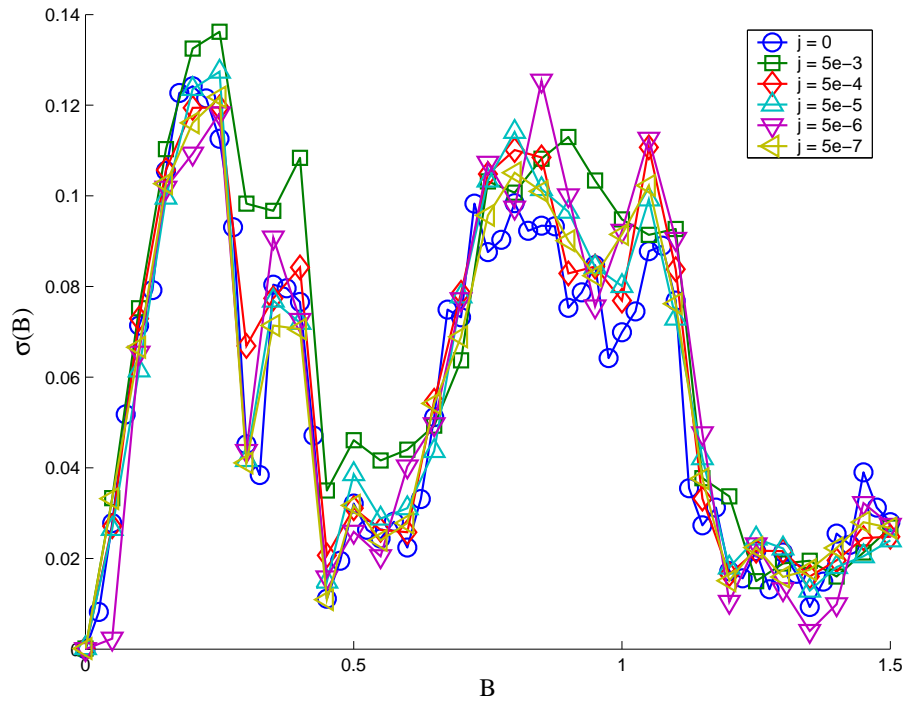


Figure 5.7: Mean Leading Lyapunov exponent in the region of small j .

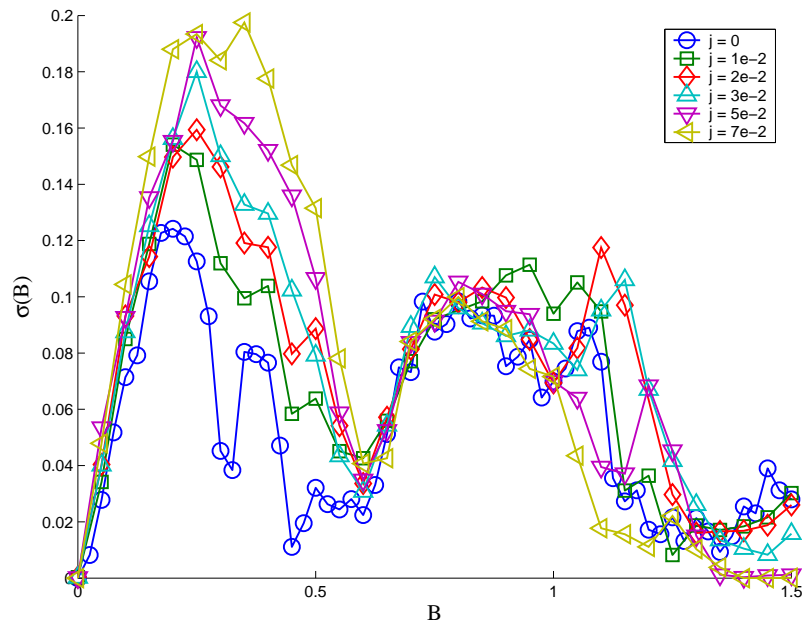
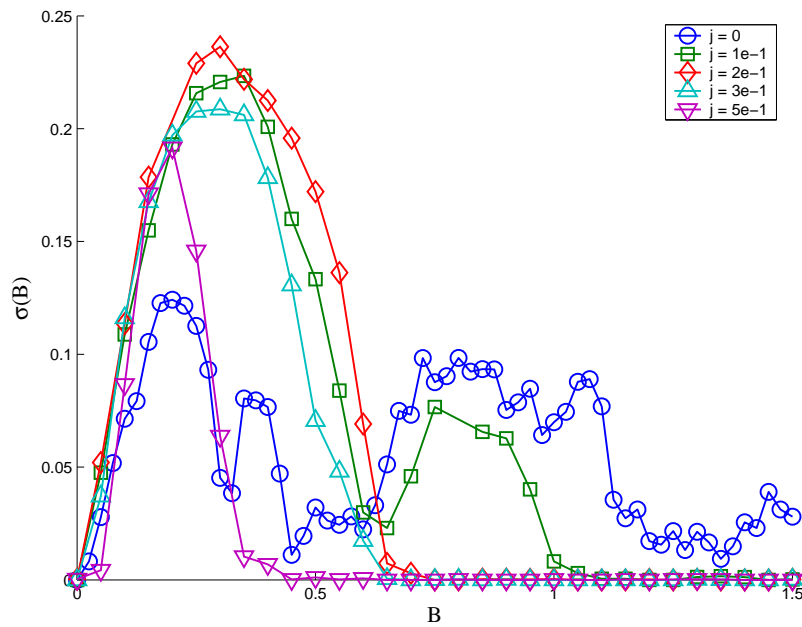


Figure 5.8: Mean Leading Lyapunov exponent in the transition region.

Figure 5.9: Mean Leading Lyapunov exponent in the region of high j .

Chapter 6

Treatise of the PAS

*“No PASaran!”*¹

The chapter focuses on the concept the Principal Axes System that was introduced in the sec. 2.2. Its existence led to the elimination of the three shape parameters $(\alpha_{21}^R, \alpha_{21}^I, \alpha_{22}^I)$. This fact might induce some false hopes about decreasing the the number of relevant shape parameters from five to two in a general case. On the contrary, it will be demonstrated that the PAS is not a very strong tool in the rotating case.

6.1 Kinematical Nature of the PAS

A question one might raise after reading sections 2.2 and 2.2.1 is whether there is *any need* for five parameters in the Lagrangian (3.1). The answer is a plain and emphatic *yes*, but its explanation is instructive.

Proposition 1 *Assume the system is transformed to the PAS at $t = 0$, so the $\alpha(0)$ matrix is diagonal. In the most general case, the $\alpha(h)$ will not be diagonal at a later time.*

Proof: Remember that the matrix of the velocities $\dot{\alpha}$ is also transformed at $t = 0$, but will not become diagonal in general. Now we should solve the equations of motion that could be derived from Lagrangian (3.1). We can avoid this work, however. Imagine *we derived* the equations. Apparently they would be like:

$$\ddot{\alpha}_{2k}^x = f(\dot{\alpha}_{2k}^x, \alpha_{2k}^x),$$

¹“No Pasaran!” meaning “They shall not pass!” was a Republican rallying cry in the Spanish Civil War.

where f would stand for the right-hand side and strange subscripts and superscripts would denote all possible indices.

Now we might to reduce the ODE of the second order into two ODEs of the first order. This can be done easily:

$$v_{\alpha_{2k}^x} \equiv \dot{\alpha}_{2k}^x.$$

Now the equations become:

$$\begin{aligned} \dot{v}_{\alpha_{2k}^x} &= f(v_{\alpha_{2k}^x}, \alpha_{2k}^x), \\ \dot{\alpha}_{2k}^x &= v_{\alpha_{2k}^x}. \end{aligned}$$

Now assume we are performing numerical solution.² We take such a small timestep h so that the right-hand-side terms are constant. Then:

$$\dot{\alpha}_{2k}^x(h) = hv_{\alpha_{2k}^x}(0).$$

So given that the velocities are non-zero at the start, as they are, even the off-diagonal α -s become *nonzero*.

Note that it does not matter what the development of the velocity is like. ■

We proved that $(\alpha_{21}^R, \alpha_{21}^I, \alpha_{22}^I)$ *cannot* be dropped, as they tend to reappear at a later time. Now we could transform the coordinates once again and eliminate the off-diagonal terms. Nonetheless, we could hardly hope they remain non-zero. So we can transform the coordinates *any time* we desire and obtain a simplified description, but we have to solve the *full equations*. This supports the notion that the coordinate transformation into the PAS is a just kinematical one.

6.2 Relevance of the PAS for the Non-Rotating Case

The previous negative results might have seriously undermined our belief in the PAS's worth. Here we will outline that all not is doom and gloom if the system lacks angular momentum.

Proposition 2 *Assume the system is transformed to the PAS at $t = 0$. Additionally, let the angular momentum be zero $\vec{J} = (0, 0, 0)$. The matrix $\alpha(t)$ will remain diagonal.*

²We are actually doing so by employing the venerable Euler method.

Proof: First of all, a zero angular momentum remains zero in all coordinate system, even in a PAS. Now recall the expression(3.8) and set the zero on the right-hand-side. We start with the third component:

$$J_3 = 2K [\dot{\alpha}_{21}^R \alpha_{21}^I - \alpha_{21}^R \dot{\alpha}_{21}^I + 2(\dot{\alpha}_{22}^R \alpha_{22}^I - \alpha_{22}^R \dot{\alpha}_{22}^I)] = 0.$$

As we are in the PAS, we can drop terms with $(\alpha_{21}^R, \alpha_{21}^I, \alpha_{22}^I)$ at $t = 0$. That means

$$-4K \alpha_{22}^R \dot{\alpha}_{22}^I = 0.$$

Now $\alpha_{22}^R(0)$ is arbitrary, so $\dot{\alpha}_{22}^I(0) = 0$. Immediately we take the terms for J_1 and J_2 .

$$J_1 = \sqrt{2}K \left[\sqrt{2}(\alpha_{21}^I \dot{\alpha}_{22}^R - \dot{\alpha}_{21}^I \alpha_{22}^R + \dot{\alpha}_{21}^R \alpha_{22}^I - \alpha_{21}^R \dot{\alpha}_{22}^I) + \sqrt{3}(\dot{\alpha}_{20} \alpha_{21}^I - \alpha_{20} \dot{\alpha}_{21}^I) \right] = 0$$

$$J_2 = \sqrt{2}K \left[\sqrt{2}(\dot{\alpha}_{21}^R \alpha_{22}^R - \alpha_{21}^R \dot{\alpha}_{22}^R + \dot{\alpha}_{21}^I \alpha_{22}^I - \alpha_{21}^I \dot{\alpha}_{22}^I) + \sqrt{3}(\dot{\alpha}_{20} \alpha_{21}^R - \alpha_{20} \dot{\alpha}_{21}^R) \right] = 0$$

We use the nullity of non-diagonal terms and $\dot{\alpha}_{22}^I$ to obtain:

$$\sqrt{2} \dot{\alpha}_{21}^I \alpha_{22}^R + \sqrt{3} \alpha_{20} \dot{\alpha}_{21}^I = 0,$$

$$\sqrt{2} \dot{\alpha}_{21}^R \alpha_{22}^R - \sqrt{3} \alpha_{20} \dot{\alpha}_{21}^R = 0.$$

Well, it is manifestly evident that for arbitrary $\alpha_{22}^R(0)$ and $\alpha_{20}(0)$ the $\dot{\alpha}_{21}^R(0)$ and $\dot{\alpha}_{21}^I(0)$ must be zero.

In sum, the initial velocities of the off-diagonal terms are zero. This ensures that the off-diagonal terms remain zero in the next step. Moreover, the condition $\vec{J} = \vec{0}$ holds for all times, so the proof above could be repeated. It would be shown that $\dot{\alpha}_{21}^R(h)$, $\dot{\alpha}_{21}^I(h)$, and $\dot{\alpha}_{22}^I(h)$ are zero. ■

Now it has been shown the $\alpha(t)$ remains diagonal in the non-rotating case. The PAS thus stays the same.³

6.3 Demonstrative Value of the PAS

We saw that the PAS cannot be used to simplify the equations of motion for the rotating case. On the other hand, the PAS has a certain demonstrative value. Remember that proper deformations are most conveniently studied in that system.

So one might propose to study the deformations while disregarding the rotations by:

³This enlightens the footnote 5 in chapter 2.

1. Solving the equations by one step for $(\alpha_{20}, \alpha_{21}^R, \alpha_{21}^I, \alpha_{22}^R, \alpha_{22}^I)$.
2. Transforming the coordinates into PAS and note either (α_0, α_2) or (β, γ) .

This would enable comparison of the deformations in the rotating and non-rotating case. Such an analysis would be quite valuable. Nonetheless, several discomfoting problems arise.

6.3.1 Coordinate Degeneracy

It has been mentioned that the choice of the PAS is not unique. Permutation of the basis vectors and inversions supply the variation. From a purely algebraical point of view this would be negligible. However, the terms in the α matrix are *marked* – we assigned them specific meaning. Therefore the permutation of the numbers on the diagonal is of *considerable* concern. For instance, the permutation of the x and y axes causes inversion in sign of α_2 and preserves α_0 , cf. (2.6).

The foreshadowed problem resurface when one tries to diagonalize the α -matrix.⁴ The routine performing the diagonalization, the LAPACK ([12]) chooses such a basis that the eigenvalues are placed on the diagonal in ascending order. This is a severe drawback – after each step, one has to verify that the last transformation matrix was “closest” to the previous one. If it was not, the closest one has to be found and appropriate transformations performed.

Not only does this procedure sound complicated, but is just so bewildering when applied. Its implementation is time-consuming and error-prone. Once this is accomplished, a startling phenomenon is encountered.

6.3.2 Abrupt Changes and Avoided Crossings

Assume that we have constructed a routine that eliminates troubles that arise from the coordinate degeneracy. Now we can start comparing the cases of zero and non-zero angular momentum.

We choose special initial conditions so that $\alpha_{22}^I(0) = 0$. This means that the system *is* in the PAS system at the start. Now we start evolving the system and transforming into the “nearest” PAS for a while. We plot the graph in the (a_0, a_2) plane.

In the next step we use the same initial conditions as above, but we eliminate

⁴The discussion is becoming a tad technical, but these steps have to be carried out in computations.

the angular momentum by setting the $\dot{\alpha}_{22}^I(0)$ to zero. We evolve the system and add results to the plot we have already drawn. A sample scenario is depicted in fig. 6.1, left panel.

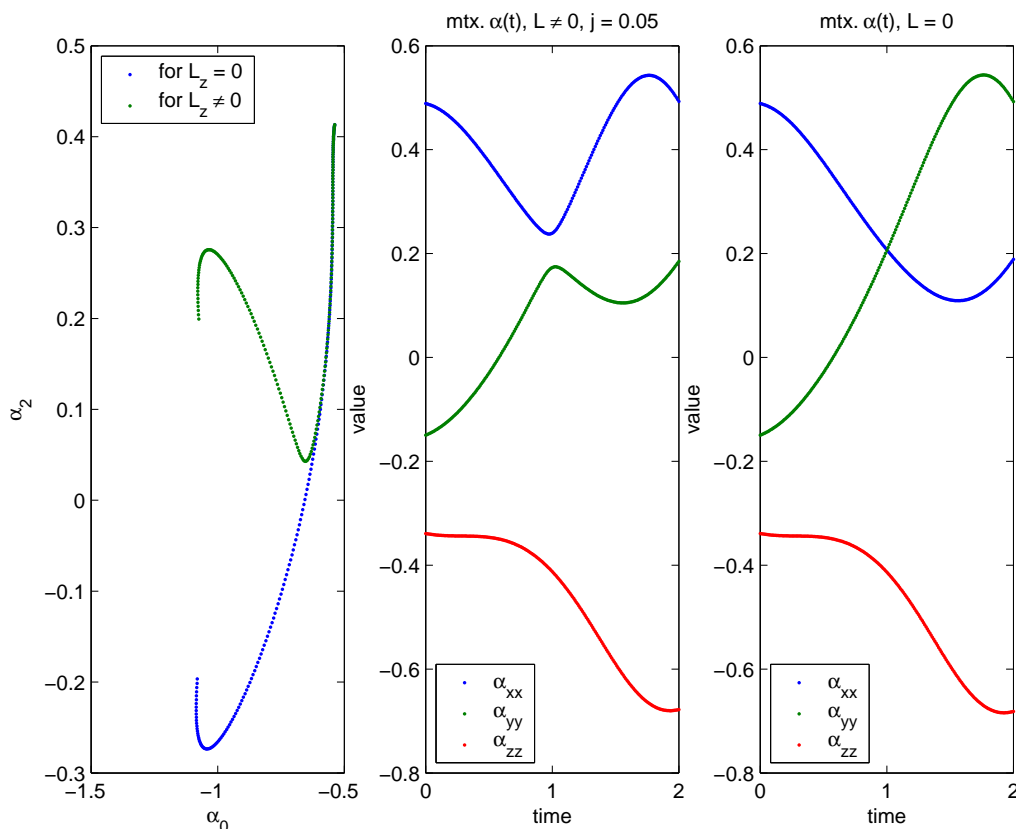


Figure 6.1: A demonstration of abrupt divergence of trajectories – left, and evolution of eigenvalues of α for both rotating and non-rotating cases – middle and right

Now it seems that something is amiss here. We might have expected a slight divergence of the trajectories, but we observe a *dramatic separation* instead. The observation is disquieting. Its causes remain a bit inexplicable, but a proposition have been put forward.

In addition to the (a_0, a_2) plots, we draw time dependence of the cartesian representation of the shape parameters, see fig. 6.1, middle and right panel. We discern the difference at once: The α_{xx} and α_{yy} do not cross in the middle panel. They rather “rebound”. So we concur that the abrupt divergence is

associated with the non-crossing of the cartesian parameters.

This conclusion does not solve the puzzle completely. The problem is rather displaced – one has to explain the cause of the avoided crossing. The task is a formidable one, for it essentially involves analysis of the time-dependence of the eigenvalues. For the purpose of this work, there has not been a substantial effort in that direction. Yet, it is certain that the phenomenon would be a suitable target of further scrutiny.

There is a hint that there might be physical, rather than mathematical reasons lurking behind the scene. The expressions (6.183) from [4] for moments of inertia might be the first step.

The question still stands: Who shall pass?

Chapter 7

Numerical Aspects

The chapter contains a simplified description and explanation of the main algorithms that have been used in the course of the work. The goal is to provide a concise but transparent picture of the method, so that the relevance of results can be questioned. For the very reason the weaker points will be emphasized and discussed. Additionally, a few important parts of the source code will be presented. Another reason is purely pedagogical, as the chapter may well be used as an introduction to numerical investigation of chaos. The algorithms could be employed to tackle new problems if suitably modified. This requires their good knowledge, however.

The listed examples feature the MATLAB¹ syntax that is very similar to the standard C notation.

7.1 Determination of the Lyapunov Exponent

The Lyapunov exponent has been defined by (4.3). Unfortunately, the definition is not suitable for direct computation. A number of sophisticated methods can be found in the literature, f.i. in [6], [7]. They might involve linearization of the equations ([6], [7]) or subtle application of functional and spectral analysis ([7]).

On the other hand, there are two useful and simpler methods that could be employed as well.

¹MATLAB is a high-level language and interactive environment developed by the Math-Works, Inc.

7.1.1 Method 1

Despite the fact that it might appear simplistic and uncomplicated, this method can be employed successfully. It was used by Alhassid and Wheelan in [2] for calculations of the the average largest Lyapunov exponent, and the fractional volume of chaotic trajectories in the classical limit of the IBM model.

Recall that Lyapunov exponent is the limit of $\ln R(t)/t$. Yet, the limit of infinite time is mightily inconvenient for several reasons. First, two trajectories cannot diverge exponentially in a bounded system for ever. Secondly, infinite time is numerically impractical. Therefore a suitable terminal time has to be chosen. If it is done shrewdly, then the behavior of the rate of divergence $\ln R(t)$ provides the distinction between regular and chaotic trajectories:

- i) The function $\ln R(t)$ is almost piecewise linear function of t . The first part has nonzero slope, while the second tends to be constant. Obviously, the first part corresponds to the divergence of trajectories, while the second is caused by the impossibility of further expansion. The Lyapunov exponent of this chaotic trajectory can be determined as the slope of its first part.
- ii) The function has logarithmic behavior which suggest that in the limit of infinite time the Lyapunov exponent will be zero. The trajectory is therefore regular.

A sample of a regular and a chaotic trajectory is shown in figure 7.1. The red lines are attempts to fit a generic chaotic dependence, while the cyan ones fit a regular dependence.

There are two points that have to be addressed, though. The first one is the choice of terminal time. The requires some knowledge of the system and has to be done semi-empirically. The other point involves tackling intermediate trajectories that defy the classification mentioned above. Additional information on the matter can be found in [2].

7.1.2 Method 2

The second method is similar, but does not provide an intrinsic criterion of regularity. It is comprehensibly described in [3], so only a brief summary will be given here.

We let the system evolve for a while ($t < T_{adv}$). Then the core idea is to compute Lyapunov exponent after *finite time*, while readjusting $\tilde{y}(t)$ so that its distance from $y(t)$ remains ε after each iteration. Precisely:

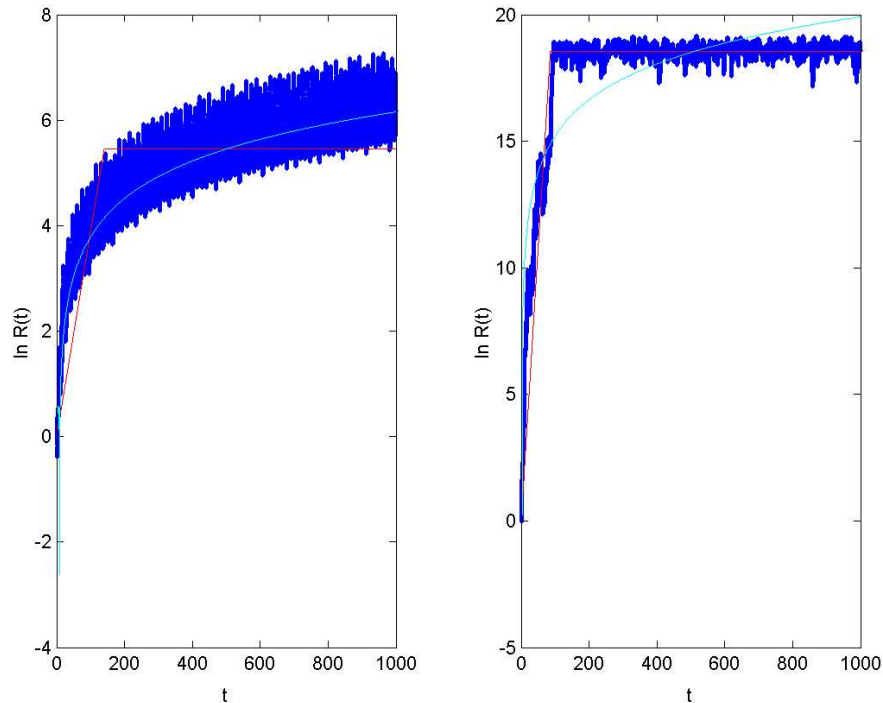


Figure 7.1: An example of a regular (left) and a chaotic (right) trajectory with attempted fits of $\ln R(t)$

```

cnt = 1;
while (t <= Tfin)
    [t, y] = RK4(t,y,h);          % advance y by one step
    [t, y_p] = RK4(t-h,y_p,h);  % advance y_p
    sgm(cnt) = log(norm(y-y_p)/eps1)/h; % calc. "L. exp"
    y_p = y + (y_p-y)/norm(y_p-y)*eps1; % readjust y_p
    cnt = cnt + 1;
end

```

The array `sgm` contains proto-Lyapunov exponents of the trajectory. Hence the final exponent is obtained as an average of the array. The method could be further elaborated.

A certain disadvantage of the method is an apparent numerical non-elegance of the readjustment. This source of possible errors can be negated by a good choice of initial separation and timestep, however. On the other hand, it has been observed that the method tends to be slightly incompatible with

adaptive stepsize. Last, the method does not involve analysis of functions as the previous one, namely one does not have to fit expected dependence, although this has its price, see section 7.3.

7.2 The Runge-Kutta Method

The section is divided into two subsections. The first one contains the basic formula for the fourth-order Runge-Kutta method and a sample code of its implementation. The second part deals with error estimation and adaptive stepsize control.

7.2.1 Basics

It has been suggested that Runge-Kutta solver has been employed. Despite the fact that the RK is a part of the standard numerical armory, its basics are repeated here for reader's convenience. More information can be looked up in literature, namely [8].

Consider a set of first-order differential equations for the functions y_i

$$\frac{dy_i(x)}{dx} = f_i(x, y_1, \dots, y_N), \quad i = 1, \dots, N,$$

assuming that the functions f_i on the right-hand side are known. For an initial value problem, the fourth-order Runge-Kutta formula is:

$$\begin{aligned} k_1 &= hf(x_n, y_n) \\ k_2 &= hf(x_n + \frac{h}{2}, y_n + \frac{k_1}{2}) \\ k_3 &= hf(x_n + \frac{h}{2}, y_n + \frac{k_2}{2}) \\ k_4 &= hf(x_n + h, y_n + k_3) \\ y_{n+1} &= y_n + \frac{k_1}{6} + \frac{k_2}{3} + \frac{k_3}{3} + \frac{k_4}{6} + \mathcal{O}(h^5). \end{aligned} \quad (7.1)$$

Sample code:²

```
t = 0; p = 1; y = y_0;
while t <= Tfin
    R(p,:) = y; p = p + 1;
    k1 = h*em3(y);
```

²Note that the functions f_i are not explicitly time-dependent, recall (3.5). So t does not have to be passed to `em3`.

```

    k2 = h*em3(y+k1/2);
    k3 = h*em3(y+k2/2);
    k4 = h*em3(y+k3);

    y = y + k1/6 + k2/3 + k3/3 + k4/6;
    t = t + h;
end
R(p,:) = y;    % The solution is stored in R(1:p,:)

```

7.2.2 Error Estimation and Adaptive Stepsize Control

The basic form of the RK (7.1) does not provide an error estimate. This has to be addressed, as the error estimate is vital for several reasons. First, we require that the results of the computation are more precise than the `eps1` that governs the separation. If the numerical error got greater than the separation, the resultant Lyapunov exponent would be erroneous. Second, even in a more general case, the error estimate is useful, especially for adaptive stepsize methods.

One way of estimating the error is the half-step method: advance y by stepsize h and advance it twice by $\frac{h}{2}$. The error estimate is then the norm of the difference:

```

[t, y_1s] = RK4(t_0,y,h);    % 1-step, full stepsize

[t, y_2s] = RK4(t_0,y,h/2); % 1st step, half stepsize
[t, y_2s] = RK4(t,y_2s,h/2); % 2nd step, half stepsize

err_est = norm(y_1s-y_2s);   % compute error estimate

```

It has been emphasized that the error estimate is invaluable and the lines above could be used to calculate it. However, note that this particular implementation adds 8 additional evaluations of the right-hand side. The greater control thus comes at its price.

Once we possess reliable means of error estimate, it may turn out that error estimate is greater than the required precision: $\Delta_{est} > \Delta_{required}$. In this case one must keep decreasing the stepsize until the required precision is attained. So it would seem that the advantage of the error estimate means just *more work* and the conviction that the method is not error-prone. On the other hand, one might *increase* the stepsize if the error is too small so that fewer steps are needed to finish the calculation. Thus the extra code and work will be repaid more than fairly by the considerably greater efficiency. [8]

Surprisingly, the adaptive stepsize method has been subject to failures in the course of testing and has been abandoned. Therefore, the error estimates have been made separately and the stepsize set to $h = 0.001$ as it was mentioned in section 7.2.1. The value has appeared to provide greater than sufficient precision throughout the testing. Consequently, the final algorithms do not feature any sort of precision checking for the sake of decreased time consumption.³ The omission of the routine remains a liability, nonetheless.

7.3 Estimation of Chaos Threshold

It has been mentioned that the crucial point is the distinction between regular and chaotic trajectories based on their Lyapunov exponents.⁴ Theoretically it is very simple: whenever a Lyapunov exponent is nonzero, the trajectory is chaotic.⁵

However, once a numerical attempt has been made, it turns out that the matter is not so simple. Figure 7.2 shows Lyapunov exponents of trajectories obtained for various energies in the analytically integrable case when $B = 0$.⁶ First of all, one observes that there are *no trajectories* with zero Lyapunov exponent. Does that mean that there are no regular trajectories? Apparently not. This disturbing fact only means that the *standard criterion* has to be adjusted. In fact, knowledge that all these trajectories *must be* regular leads our way.

The straight-forward idea is that the trajectories whose Lyapunov exponent is smaller than a certain non-zero – empirically obtained number – will be considered regular. The critical number will be computed as the maximum from a large number of Lyapunov exponents for the fully integrable case. Its resultant value is:⁷

$$\sigma_{\text{threshold}} \doteq 0.01671.$$

It is good to remind that the non-zero value of the threshold stems from the employed method. The value is significantly dependent of the T_{clc} ⁸, the computational time and not so much on the h , the stepsize of the Runge-Kutta. However, an excessive minimization of $\sigma_{\text{threshold}}$ is too costly, as both

³Cf. (7.4) and realize that 8 additional evaluations per step would result in threefold required time.

⁴This section concerns Method 2.

⁵Cf. section 4.2 for details.

⁶This case will be referred to further as *fully integrable* with the idea of emphasizing that there are only regular trajectories in the phase space.

⁷For $T_{adv} = 75$, $T_{clc} = 500$, $h = 0.001$.

⁸For $T_{adv} \simeq 50$, $T_{clc} = 250$, $h = 0.001$ the $\sigma_{\text{threshold}} \doteq 0.021$.

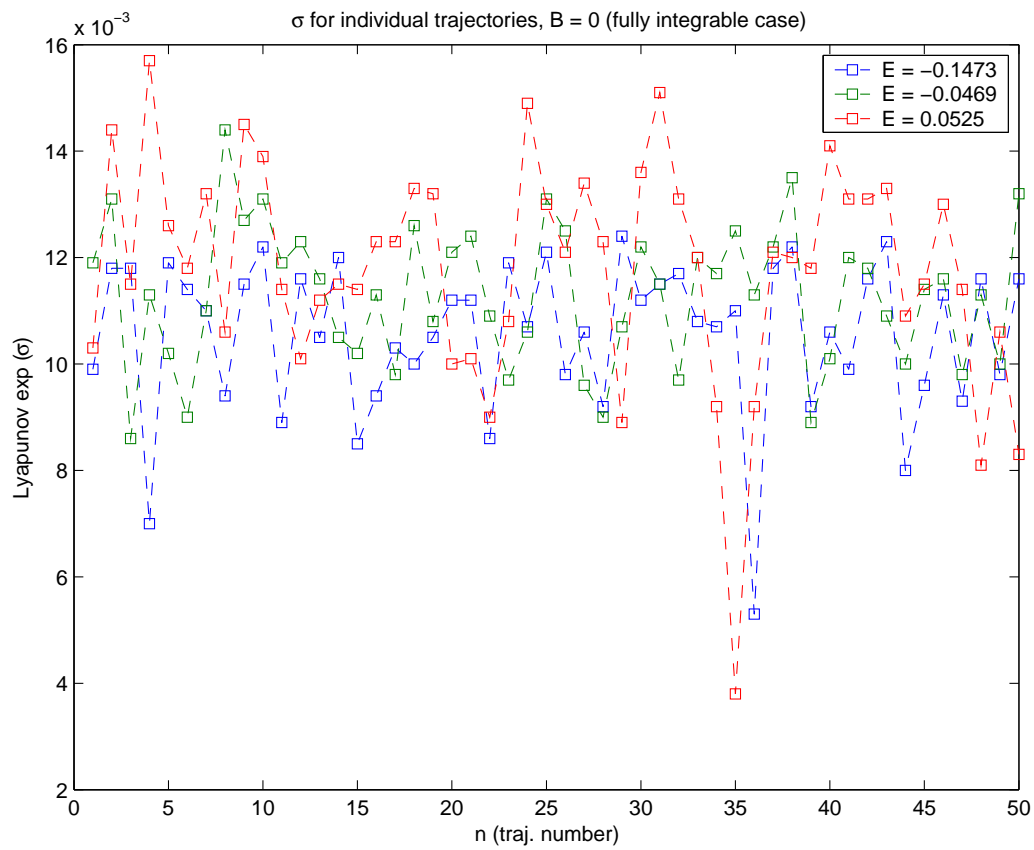


Figure 7.2: A sample demonstrating the non-vanishing values of σ for trajectories in the fully integrable case

an increase in T_{calc} and a decrease in h result in greater time and memory consumption.

Last, a typical value of average largest σ is greater than $\sigma_{\text{threshold}}$ by a factor of 2-3 at least. That is reassuring for the method, as it shows that not many trajectories exist in the *grey zone*, where their status would be dubious.

7.4 Computational Time

The following section⁹ does not contain any purely scientific results, but it is worth some attention. Even the most elaborate theoretical concept has to be implemented lest it becomes an inutile fancy relic.

Inevitably, the time required to perform the calculations could be the limiting factor of the described methods. A simple count is therefore provided.

Figures 5.2-5.4 feature approximately 31 points per line. Each point is an average of 100 trajectories. A single trajectory takes approximately 118-150 s to evaluate. This makes it 3h:16-4h:10 per point. Clearly, a single line totals roughly 102-129 h, at most a little more than 5 days.¹⁰

These estimates suggest that all computation could be performed in a matter of week or fortnight if half-dozen computers were employed. This was indeed the case. On the other hand, the required time justifies the number of crude estimates and simplifications that have been carried out – the rejection of the error checking in particular. See sect. 7.2.2.

Additionally, the time requirements demonstrate that the matter is fairly demanding on both hardware and algorithms. Eventually, if subsequent attempts to verify and elaborate the results are to be attempted, a shift from MATLAB is advisable.

⁹The estimates were calculated for Method 2.

¹⁰The given numbers apply to for the following configurations: *PC (x86-64) AMD 64 3200+ (2.2GHz) - socket 754, 1024 MB RAM, Gentoo Linux* and *PC (x86) Pentium 4 2,6/2,8/3 GHz, 512/1024 MB RAM - dual channel Gentoo Linux*. No sluggards.

Appendix A

Constants of Motion and Integrability

A.1 The Non-rotating Case

We recall the old Lagrangian (1.1):

$$\mathcal{L} = \frac{K}{2}(\dot{\beta}^2 + \beta^2\dot{\gamma}^2) - A\beta^2 - B\beta^3 \cos(3\gamma) - C\beta^4.$$

We would like to find the integrals of motion the system possesses and discuss its integrability.

Assume that $B=0$. Moreover, for the sake of the analysis let us get rid of the constants A , C , and K by setting them to 1.

$$\mathcal{L} = \frac{1}{2}(\dot{\beta}^2 + \beta^2\dot{\gamma}^2) - \beta^2 - \beta^4.$$

Apparently, γ is a cyclic coordinate, so

$$I_1 = \frac{\partial \mathcal{L}}{\partial \dot{\gamma}} = \beta^2 \dot{\gamma}$$

is an integral of motion. Moreover, the Lagrangian is time independent, so energy will be conserved as well. We re-write the the expressions by Hamiltonian formalism.

The canonical momenta are:

$$\pi_\beta = \dot{\beta}, \quad \pi_\gamma = \beta^2 \dot{\gamma}.$$

Additionally, the latter is equal to the recently-found integral of motion.

The Hamiltonian will become:

$$\mathcal{H} = \frac{1}{2} \left(\pi_\beta^2 + \frac{\pi_\gamma^2}{\beta^2} \right) - \beta^2 - \beta^4.$$

In order to verify that I_1 (angular momentum) and \mathcal{H} (energy) are compatible, we have to check whether their Poisson bracket vanishes.

$$\{I_1, \mathcal{H}\}_{Poisson} = \left\{ \pi_\gamma, \frac{1}{2} \left(\pi_\beta^2 + \frac{\pi_\gamma^2}{\beta^2} \right) - \beta^2 - \beta^4 \right\}$$

As π_γ, π_β are canonical momenta and β is a canonical coordinate, the first, third and fourth terms are inevitably zero.

The remaining one vanishes as well:

$$\begin{aligned} \left\{ \pi_\gamma, \frac{1}{2} \left(\frac{\pi_\gamma^2}{\beta^2} \right) \right\} &= \frac{\partial \pi_\gamma}{\partial \beta} \frac{\partial \left(\frac{\pi_\gamma^2}{\beta^2} \right)}{\partial \pi_\beta} - \frac{\partial \pi_\gamma}{\partial \pi_\beta} \frac{\partial \left(\frac{\pi_\gamma^2}{\beta^2} \right)}{\partial \beta} + \frac{\partial \pi_\gamma}{\partial \gamma} \frac{\partial \left(\frac{\pi_\gamma^2}{\beta^2} \right)}{\partial \pi_\gamma} - \frac{\partial \pi_\gamma}{\partial \pi_\gamma} \frac{\partial \left(\frac{\pi_\gamma^2}{\beta^2} \right)}{\partial \gamma} = \\ &= 0 - 0 + 0 - 0 = 0. \end{aligned}$$

We have proven that I_1 and \mathcal{H} are in involution. There are clearly functionally independent as well. Once we recall the definition of the integrable system (section 4.1), we conclude that the system described by Lagrangian (1.1) is integrable if $B = 0$. On the other hand, if the parameter is non-zero, the expression I_1 will not be a constant of motion any longer. This suggests that the system is chaotic.

A.2 The Rotating Case

Unlike in the previous paragraph, we will start with a cartesian form. The Lagrangian we derived was (3.3):

$$\mathcal{L} = \frac{K}{2}(\dot{\eta}^2 + \dot{\xi}^2 + \dot{\zeta}^2) - A(\eta^2 + \xi^2 + \zeta^2) + B\eta[3(\xi^2 + \zeta^2) - \eta^2] - C(\eta^2 + \xi^2 + \zeta^2)^2.$$

As above, we set $B = 0$ and $-A = C = K = 1$, and so we obtain the Hamiltonian:

$$\mathcal{H} = \frac{1}{2}(\pi_\eta^2 + \pi_\xi^2 + \pi_\zeta^2) + (\eta^2 + \xi^2 + \zeta^2) + (\eta^2 + \xi^2 + \zeta^2)^2.$$

The problem appears to be spherically symmetric, so the angular momenta will should be integrals of motion. We define them canonically:

$$\begin{aligned} J_\eta &\equiv \xi \pi_\zeta - \pi_\xi \zeta, \\ J_\xi &\equiv \zeta \pi_\eta - \pi_\zeta \eta, \\ J_\zeta &\equiv \eta \pi_\xi - \pi_\eta \xi. \end{aligned}$$

The square of the magnitude, J^2 is thus:

$$J^2 = \eta^2 \pi_\xi^2 + \eta^2 \pi_\zeta^2 + \xi^2 \pi_\eta^2 + \xi^2 \pi_\zeta^2 + \zeta^2 \pi_\eta^2 + \zeta^2 \pi_\xi^2 - 2(\eta \pi_\eta \xi \pi_\xi + \eta \pi_\eta \zeta \pi_\zeta + \xi \pi_\xi \zeta \pi_\zeta).$$

We verify that the angular momentum is an integral of motion:

$$\begin{aligned} \{\mathcal{H}, J_\eta\} &= \frac{\partial \mathcal{H}}{\partial \eta} \frac{\partial J_\eta}{\partial \pi_\eta} - \frac{\partial \mathcal{H}}{\partial \pi_\eta} \frac{\partial J_\eta}{\partial \eta} + \frac{\partial \mathcal{H}}{\partial \xi} \frac{\partial J_\eta}{\partial \pi_\xi} - \frac{\partial \mathcal{H}}{\partial \pi_\xi} \frac{\partial J_\eta}{\partial \xi} + \frac{\partial \mathcal{H}}{\partial \zeta} \frac{\partial J_\eta}{\partial \pi_\zeta} - \frac{\partial \mathcal{H}}{\partial \pi_\zeta} \frac{\partial J_\eta}{\partial \zeta} = \\ &= 2\xi[1 + 2(\eta^2 + \xi^2 + \zeta^2)](-\zeta) - \pi_\eta \pi_\zeta + \\ &+ 2\zeta[1 + 2(\eta^2 + \xi^2 + \zeta^2)](\xi) + \pi_\zeta \pi_\xi = 0. \end{aligned}$$

So the η -component of the angular momentum is a compatible integral of motion. The cyclic permutation $\eta \rightarrow \xi \rightarrow \zeta$ would allow us to prove the same for both J_ξ and J_ζ . On the other hand, we cannot expect that the components of the angular momentum are in involution with one another. The proof of compatibility for \mathcal{H} and J^2 is similar:

$$\begin{aligned} \{\mathcal{H}, J^2\} &= 4\eta[1 + (\eta^2 + \xi^2 + \zeta^2)][\pi_\eta(\xi^2 + \zeta^2) - \eta(\pi_\xi \xi + \pi_\zeta \zeta)] - 2\pi_\eta[\eta(\pi_\xi^2 + \pi_\zeta^2) - \pi_\eta(\pi_\xi \xi + \pi_\zeta \zeta)] \\ &+ 4\xi[1 + (\eta^2 + \xi^2 + \zeta^2)][\pi_\xi(\eta^2 + \zeta^2) - \xi(\pi_\eta \eta + \pi_\zeta \zeta)] - 2\pi_\xi[\xi(\pi_\eta^2 + \pi_\zeta^2) - \pi_\xi(\pi_\eta \eta + \pi_\zeta \zeta)] \\ &+ 4\zeta[1 + (\eta^2 + \xi^2 + \zeta^2)][\pi_\zeta(\eta^2 + \xi^2) - \zeta(\pi_\eta \eta + \pi_\xi \xi)] - 2\pi_\zeta[\zeta(\pi_\eta^2 + \pi_\xi^2) - \pi_\zeta(\pi_\eta \eta + \pi_\xi \xi)] \\ &= 4[1 + (\eta^2 + \xi^2 + \zeta^2)] \times \\ &\times [\eta \pi_\eta(\xi^2 + \zeta^2) - \eta^2(\pi_\xi \xi + \pi_\zeta \zeta) + \xi \pi_\xi(\eta^2 + \zeta^2) - \xi^2(\pi_\eta \eta + \pi_\zeta \zeta) + \zeta \pi_\zeta(\eta^2 + \xi^2) - \zeta^2(\pi_\eta \eta + \pi_\xi \xi)] \\ &- 2[\eta \pi_\eta(\pi_\xi^2 + \pi_\zeta^2) - \pi_\eta^2(\pi_\xi \xi + \pi_\zeta \zeta) + \xi \pi_\xi(\pi_\eta^2 + \pi_\zeta^2) - \pi_\xi^2(\pi_\eta \eta + \pi_\zeta \zeta) + \zeta \pi_\zeta(\pi_\eta^2 + \pi_\xi^2) - \pi_\zeta^2(\pi_\eta \eta + \pi_\xi \xi)] \\ &= 0. \end{aligned}$$

The same can be done for J_η and J^2 :

$$\begin{aligned} \{J_\eta, J^2\} &= 2\pi_\zeta[\pi_\xi(\eta^2 + \zeta^2) - \xi(\eta \pi_\eta + \zeta \pi_\zeta)] + 2\zeta[\xi(\pi_\eta^2 + \pi_\zeta^2) - \pi_\xi(\eta \pi_\eta + \zeta \pi_\zeta)] - \\ &- 2\pi_\xi[\pi_\zeta(\eta^2 + \xi^2) - \zeta(\eta \pi_\eta + \xi \pi_\xi)] - 2\xi[\zeta(\pi_\eta^2 + \pi_\xi^2) - \pi_\zeta(\eta \pi_\eta + \xi \pi_\xi)] = \\ &= 0. \end{aligned}$$

We have proven that there exist three independent and compatible constants of motion: \mathcal{H}, J^2, J_η . The conclusion is that the system is again integrable, if $B = 0$. With the non-zero value of B , the system loses rotational invariance, and as a consequence some integrals of motion. So we deduce that it will be chaotic.

Appendix B

Analysis of $J_{max}(E, B)$

Since the beginning of this work we have encountered the j , the fraction of J and J_{max} . However, the properties of the denominator J_{max} have not been mentioned so far. Yet, the determination of maximal angular momentum for a given energy and B^1 is an interesting exercise.

We have to find an extremum of the function J_3 while satisfying the energy constraint at the same time. The method of Lagrange multipliers is therefore a natural choice. Before its application, we make a few preparatory steps.

We recast the Hamiltonian (3.4) into cylindrical coordinates:

$$\mathcal{H} = \frac{1}{2K}(\pi_R^2 + \pi_\varphi^2/R^2 + \pi_z^2) + A(R^2 + z^2) - Bz(3R^2 - z^2) + C(R^2 + z^2)^2.$$

We use the scaling ($-A = K = C = 1$) and obtain:

$$\mathcal{H} = \frac{1}{2}(\pi_R^2 + \pi_\varphi^2/R^2 + \pi_z^2) - (R^2 + z^2) - Bz(3R^2 - z^2) + (R^2 + z^2)^2.$$

We also rewrite the expression for angular momentum, namely J_3 into cylindrical coordinates. This is straightforward and leads to: $J_3 = -2\pi_\varphi$.

Assume we want to maximize J_3 for a certain energy. Let us construct a new function: $F \equiv J_3 + \lambda(\mathcal{H} - E)$. We will attempt to find extrema of this

¹We will employ the standard scaling.

function. So we begin:

$$\begin{aligned}
\frac{\partial F}{\partial \pi_R} &= \lambda \pi_R = 0 \\
\frac{\partial F}{\partial \pi_z} &= \lambda \pi_z = 0 \\
\frac{\partial F}{\partial \pi_\varphi} &= -2 + \lambda(\pi_\varphi/R^2) = 0 \\
\frac{\partial F}{\partial R} &= \lambda[-\pi_\varphi^2/R^3 - 2R - 6BzR + 4R(R^2 + z^2)] = 0 \\
\frac{\partial F}{\partial z} &= \lambda[-2z - 3B(R^2 - z^2) + 4z(R^2 + z^2)] = 0 \\
\frac{\partial F}{\partial \varphi} &= 0 = 0 \\
\frac{\partial F}{\partial \lambda} &= 1/2(\pi_R^2 + \pi_\varphi^2/R^2 + \pi_z^2) - (R^2 + z^2) - Bz(3R^2 - z^2) + (R^2 + z^2)^2 - E = 0
\end{aligned}$$

We immediately recognize that $\lambda \neq 0$ as a result of the third equation. So we may all other equations by λ . This promptly brings:

$$\begin{aligned}
\pi_R &= \pi_z = 0 \\
\pi_\varphi &= 2R^2/\lambda \\
-\pi_\varphi^2/R^3 - 2R - 6BzR + 4R(R^2 + z^2) &= 0 \\
-2z - 3B(R^2 - z^2) + 4z(R^2 + z^2) &= 0 \\
1/2(\pi_R^2 + \pi_\varphi^2/R^2 + \pi_z^2) - (R^2 + z^2) - Bz(3R^2 - z^2) + (R^2 + z^2)^2 - E &= 0
\end{aligned} \tag{B.1}$$

We will use the first two lines to simplify the others. Supposing $R \neq 0$, we calculate the R^2 from the fourth and λ^2 from the third equation:

$$\begin{aligned}
R^2 &= \frac{-4z^3 - 3Bz^2 + 2z}{4z - 3B} \\
\lambda^2 &= \frac{2}{2(R^2 + z^2) - 3Bz - 1}
\end{aligned}$$

We plug R^2 into λ^2 :

$$\begin{aligned}
R^2 &= \frac{-4z^3 - 3Bz^2 + 2z}{4z - 3B} \\
\lambda^2 &= \frac{2(4z - 3B)}{3B(-8z^2 + 3Bz + 1)}
\end{aligned}$$

Finally we put all partial expressions together and plug them into eq. (B.1). This is an arduous task and we may well require some numerical aid. Once the calculation is done, are delighted to see a polynomial equation for z :

$$160Bz^5 + 48B^2z^4 - B(45B^2 + 84)z^3 - (4 + 16E - 9B^2)z^2 + 12B(2B + 1)z - 9EB^2 = 0$$

We cannot hope to solve the equation by hand for all B and E , but this is hardly inconvenient. Numerical solution of the the polynomials is a feature of all contemporary numerical tools. Once we have z , we swiftly calculate R , λ and eventually find the extremal J_3 . Note, however that there is much more work to be done if one wanted solve the problem completely.

We could have opted for the numerical from the beginning. If we do so, we will obtain the following graph:

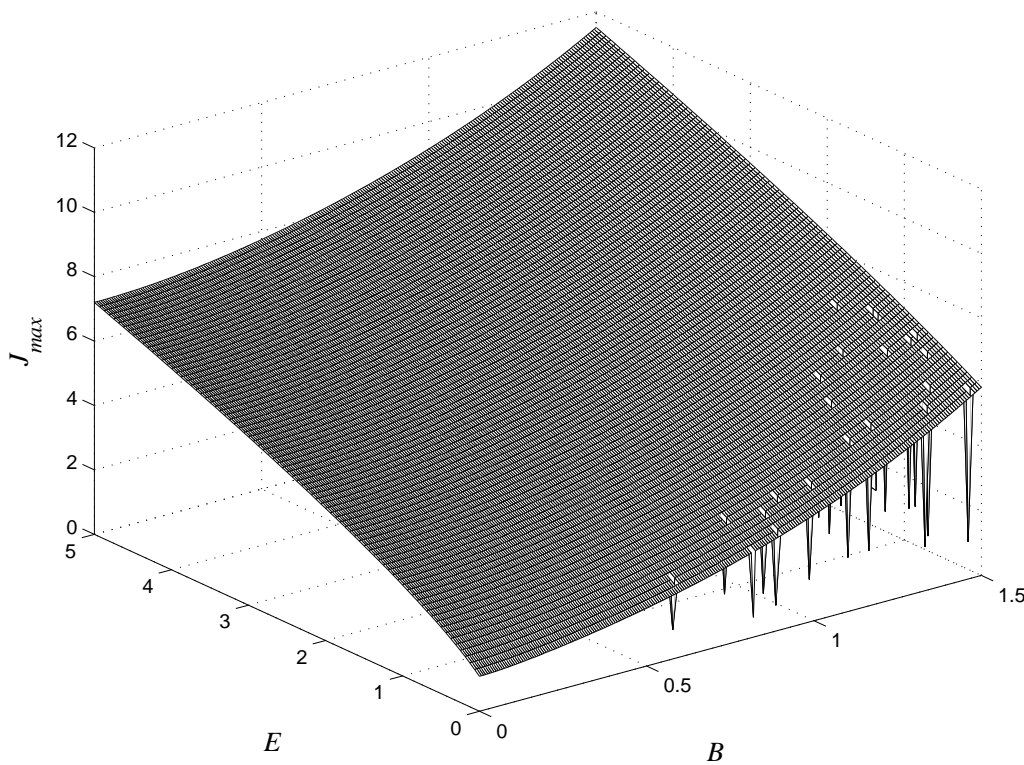


Figure B.1: $J_{max}(E,B)$

Bibliography

- [1] P. Stránský: Fázové přechody v geometrických a bosonových jaderných modelech, ÚTF MFF UK Praha, 2004
- [2] Y. Alhassid, N. Whelan: Chaos in the low-lying collective states of even-even nuclei: Classical limit; Phys. Rev. C 43, 2637–2647 (1991)
- [3] <http://sprott.physics.wisc.edu/chaos/lyapexp.htm>
- [4] W. Greiner, J. A. Maruhn: Nuclear Models; Springer, Berlin, Heidelberg, 1996
- [5] M. C. Gutzwiller: Chaos in Classical and Quantum Mechanics; Springer-Verlag, New York, 1990
- [6] S. J. Feingold, A. Peres: Linear stability test for Hamiltonian orbits; Phys. Rev. A 26, 2368–2377 (1982)
- [7] P. Cvitanović et al.: Classical and Quantum Chaos (version 10); www.nbi.dk/ChaosBook, 2003
- [8] W. H. Press, B. P. Flannery, S. A. Teukolsky, W. T. Vetterling: Numerical Recipes in C: The Art of Scientific Computing; Cambridge University Press, 1992, (www.nr.com)
- [9] A. Bohr, Kgl. Danske Videnskab Selskab Mat.-Fys. Medd. 26 No. 14 (1953)
- [10] A. Bohr, B. Motellson, Kgl. Danske Videnskab Selskab Mat.-Fys. Medd. 27 No. 16 (1953)
- [11] A. Faessler, W. Greiner, Z. Physik 168, 425 (1962)
- [12] E. Anderson, Z. Bai, C. Bischof, S. Blackford, J. Demmel, J. Dongarra, J. Du Croz, A. Greenbaum, S. Hammarling, A. McKenney, D. Sorensen: LAPACK User's Guide, Third Edition, SIAM, Philadelphia, 1999